AD-A072 566 DYNAMICS TECHNOLOGY INC TORRANCE CA F/G 20/4
RE-ESTABLISHMENT OF LAMINAR FLOW ON A HEATED SUBMERGED VEHICLE.--ETC(U)
JUL 79 E RESHOTKO, R L GRAN, K T TZOU N00014-77-C-0005
UNCLASSIFIED DT-7802-10 NL

| OF |
AD
A072566

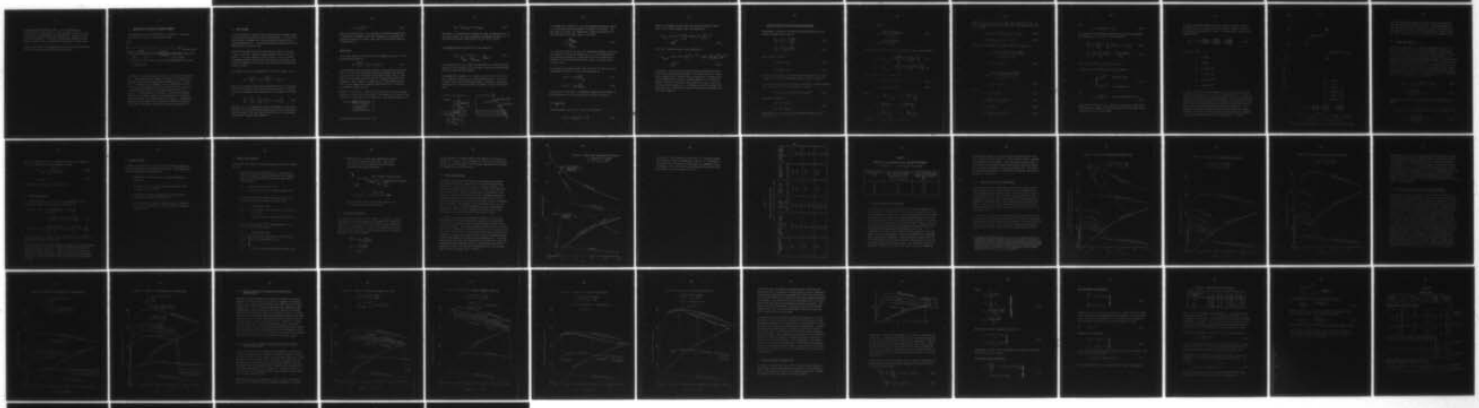

END
DATE
FILMED
9-79
DDC

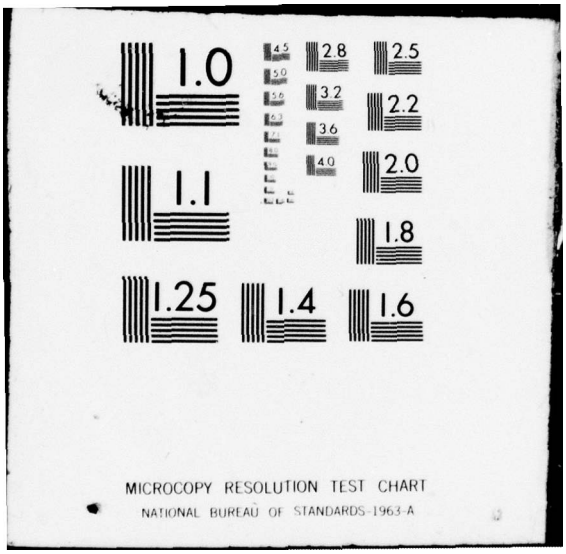
1.0
1.1
1.25
1.4
1.6
1.8
2.0
2.2
2.5
2.8
3.2
3.6
4.0
4.5
5.0
MICROCOPY RESOLUTION TEST CHART
NATIONAL BUREAU OF STANDARDS-1963-A

Dynamics Technology, Inc.

DT-7802-10

RE-ESTABLISHMENT OF LAMINAR FLOW ON A HEATED SUBMERGED VEHICLE

JUNE 1979

BY: E. RESHOTKO
R. L. GRAN
K. T. S. TZOU

SUPPORTED BY: DEFENSE ADVANCED RESEARCH PROJECTS AGENCY
AND OFFICE OF NAVAL RESEARCH
CONTRACT N00014-77-C-0005 (P0002)

DYNAMICS TECHNOLOGY, INC.
3838 CARSON STREET, SUITE 110
TORRANCE, CALIFORNIA 90503
(213) 540-5557

DISCLAIMER NOTICE

THIS DOCUMENT IS BEST QUALITY PRACTICABLE. THE COPY FURNISHED TO DDC CONTAINED A SIGNIFICANT NUMBER OF PAGES WHICH DO NOT REPRODUCE LEGIBLY.

Unclassified

SECURITY CLASSIFICATION OF THIS PAGE (When Data Entered)

REPORT DOCUMENTATION PAGE		READ INSTRUCTIONS BEFORE COMPLETING FORM
1. REPORT NUMBER DT-7802-10	2. GOVT ACCESSION NO.	3. RECIPIENT'S CATALOG NUMBER
4. TITLE (and Subtitle) Re-establishment of Laminar Flow on a Heated Submerged Vehicle		5. TYPE OF REPORT & PERIOD COVERED Technical Report
		6. PERFORMING ORG. REPORT NUMBER DT-7802-10
7. AUTHOR(s) E. Reshotko, R.L. Gran and K.T.S. Tzou		8. CONTRACT OR GRANT NUMBER(s) Contract N00014-77-C-0005 (P002)
9. PERFORMING ORGANIZATION NAME AND ADDRESS Dynamics Technology, Inc. 3838 Carson Street, Suite 110 Torrance, California 90503		10. PROGRAM ELEMENT, PROJECT, TASK AREA & WORK UNIT NUMBERS NR 062-565
11. CONTROLLING OFFICE NAME AND ADDRESS Office of Naval Research, Dept. of the Navy 800 Quincy Street Arlington, VA 22217		12. REPORT DATE July 1979 13. NUMBER OF PAGES 49
14. MONITORING AGENCY NAME & ADDRESS (if different from Controlling Office)		15. SECURITY CLASS. (of this report) Unclassified 15a. DECLASSIFICATION/DOWNGRADING SCHEDULE

16. DISTRIBUTION STATEMENT (of this Report)

Approved for Public Release; Distribution Unlimited.

17. DISTRIBUTION STATEMENT (of the abstract entered in Block 20, if different from Report)

18. SUPPLEMENTARY NOTES

19. KEY WORDS (Continue on reverse side if necessary and identify by block number)

Boundary-Layer Flow
Transition
Heated wall

20. ABSTRACT (Continue on reverse side if necessary and identify by block number)

In order to study the process by which laminar flow is re-established after a heated submerged vehicle encounters a patch of turbulent flow, an analytical model has been formulated which simulates the heat transfer characteristics of the external skin and internal heating passage of such a vehicle. This model considers the energy equations for the external skin and for the internal heating passage and the coupling between them due to heat transfer to the external flow. Numerical solutions to this coupled set of equations for a number of turbulent patch scenarios have been obtained by an explicit finite-difference procedure for a two-dimensional flat-plate

DD FORM 1473 (FACSIMILE)

393 137

Unclassified

SECURITY CLASSIFICATION OF THIS PAGE (When Data Entered)

20. ABSTRACT (continued)

example that quantitatively simulates the characteristics of a typical tow-tank test vehicle.

The maintenance of steady laminar flow on a heated submerged vehicle requires that the external surface temperature at every location along the vehicle be equal to or greater than that required to delay transition. The ability of the vehicle to recover laminar flow is sensitive to the amount by which the wall temperature exceeds the minimum required for laminar flow. If there were no temperature excess, the recovery time would be infinite. When there is excess temperature, the recovery time depends on the extent to which the turbulent event has lowered the skin temperature, and is characterized by a time constant that is directly proportional to the heat capacity per unit are of the skin and the heating fluid together and inversely proportional to the laminar heat loss rate to the external flow.

For the calculated cases, if an encountered patch of turbulence extends the order of three or more vehicle lengths, the recovery time for reasonable temperature excesses is of the order of one to three characteristic times (1/2 to 2 minutes for the cases calculated). For momentary losses of laminar flow, recovery occurs very soon after the turbulence is swept past the trailing edge.

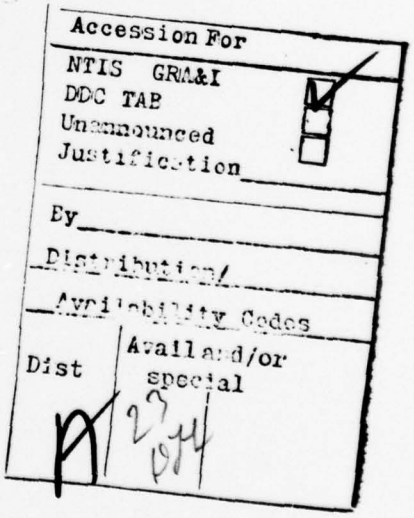

ABSTRACT

In order to study the process by which laminar flow is re-established after a heated submerged vehicle encounters a patch of turbulent flow an analytical model has been formulated which simulates the heat transfer characteristics of the external skin and internal heating passage of such a vehicle. This model considers the energy equations for the external skin and for the internal heating passage and the coupling between them due to heat transfer to the external flow. Numerical solutions to this coupled set of equations for a number of turbulent patch scenarios have been obtained by an explicit finite-difference procedure for a two-dimensional flat-plate example that quantitatively simulates the characteristics of a typical tow-tank test vehicle.

The maintenance of steady laminar flow on a heated submerged vehicle requires that the external surface temperature at every location along the vehicle be equal to or greater than that required to delay transition. The ability of the vehicle to recover laminar flow is sensitive to the amount by which the wall temperature exceeds the minimum required for laminar flow. If there were no temperature excess, the recovery time would be infinite. When there is excess temperature, the recovery time depends on the extent to which the turbulent event has lowered the skin temperature, and is characterized by a time constant that is directly proportional to the heat capacity per unit area of the skin and the heating fluid together and inversely proportional to the laminar heat loss rate to the external flow.

For the calculated cases, if an encountered patch of turbulence extends the order of three or more vehicle lengths, the recovery time for reasonable temperature excesses is of the order of one to three characteristic times (1/2 to 2 minutes for the cases calculated). For momentary losses of laminar flow, recovery occurs very soon after the turbulence is swept past the trailing edge.

TABLE OF CONTENTS

LIST OF FIGURES

LIST OF TABLES

1. INTRODUCTION

In recent years, there has been a resurgence of interest in attempting to improve a vehicle's performance by increasing the length of laminar flow in its external boundary layer. By delaying the onset of turbulence (known as Laminar Flow Control or LFC), the total drag of the vehicle may be reduced which, in turn, would allow either the use of a smaller propulsion system for a given mission or for an extended range or top speed for a given propulsion system. A number of techniques for increasing the extent of laminar flow have been identified such as vehicle shaping (wherein a favorable pressure gradient along the vehicle delays the tendency for the laminar boundary layer to undergo transition to turbulence) and suction of the boundary layer fluid through the vehicle skin. For submersible vehicles (as opposed to airships) the technique of heating the vehicle surface also has been found to delay transition because of the temperature-viscosity behavior of water. This latter technique has the added attraction that waste heat from the vehicle's propulsion system might be made available to heat the vehicle surface rather than simply being exhausted overboard; thus an increased laminar flow length might be obtainable at little or no added expenditure of power (Reference 1). Experimental research is in progress to determine how much of the theoretical performance increase is actually achievable. Systems studies are also being conducted to determine if sufficient waste heat is available and, if not, how it might be supplemented without seriously affecting vehicle design goals.

One aspect of the Laminar Flow Control area that has not, as yet, received much attention has to do with the recovery of laminar flow once it has been partially or totally lost. For example, any submerged vehicle will occasionally encounter isolated regions of turbulence (the oceanographic equivalent of clear air turbulence) or the laminar boundary layer flow may be disrupted by the adherence of a particle to the vehicle surface - thus acting as a temporary boundary layer

"trip". There is even the possibility that such a particle may simply disrupt the boundary layer flow and create a turbulent "spot" which is swept along in the boundary layer across the vehicle's surface. The loss of laminar flow is especially crucial for a heated vehicle since turbulent heat transfer rates are so much greater than laminar rates that the vehicle can, in effect, lose its overheat. Depending on the vehicle's heating system and overall heat capacity, a considerable amount of time may be required before it can heat up again and re-establish laminar flow. The modeling and calculation of such an occurrence is the subject of the present report.

Because this is the first time (to the authors' knowledge) that the laminar flow recovery problem has been analytically addressed (see Reference 2 for a qualitative description of the laminar flow recovery), the modeling employed in the present report is quite simplified in order to accentuate the basic features associated with the thermal recovery by a vehicle after a loss of laminar flow. Thus, instead of a shaped body, we have computed the recovery process on a flat-plate so as to avoid the complications introduced by pressure gradients, especially the influence of pressure gradients on estimating where boundary layer transition would occur during the recovery stage. The flat-plate configuration also allows fairly accurate estimates of even the local transient heat transfer rates during the recovery process for either laminar or turbulent flows.

Another simplification which has been employed herein is the assumption that the vehicle is heated by an internal fluid flow system in which heated water (possibly from the vehicle's propulsion plant) is pumped up to the bow of the vehicle and then toward the aft and in contact with the outer surface. This heating configuration is envisioned as a likely candidate from an engineering standpoint although other heating schemes may be as feasible (viz, electrical). Again, to avoid unnecessary complications, the heating fluid passage is assumed

to be of uniform height here despite the fact that present-day experimental vehicles have a varying channel height in order to "tailor" the local heat flux along the vehicle surface to match some other requirements.

A third simplification which has been introduced into the present analytical model is the assumption that the vehicle speed remains constant throughout the period of laminar flow recovery. Thus, the present results are applicable to the situation where a vehicle is towed through the water at a constant speed. The drag increase which accompanies the loss of laminar flow and which would cause a speed decrease in an operational situation could be incorporated at some later time. Such a consideration obviously would involve a knowledge of the vehicle's propulsion system characteristics as well as fairly accurate estimates of the parasitic drag increments during and subsequent to the loss of laminar flow. The slowing down of the vehicle caused by a loss of laminar flow would have the effect of shortening the laminar flow recovery time since the natural boundary-layer transition location and the heat flux from the vehicle both change with vehicle speed. Thus, the present estimates for laminar flow recovery are probably conservative.

In order to maintain some semblance with present-day heated vehicle designs, a composite material outer wall for the vehicle has been retained in the present analytical model. A uniform metallic vehicle skin would have been simpler to model but, aside from the problems of physically maintaining the integrity of such a skin (i.e., problems associated with corrosion, pitting, wetting, etc.), a composite material surface (such as a ceramic coating on a copper substrate) has the advantage of having a high heat capacity combined with an insulating effect to ameliorate the chilling which accompanies a sudden burst of turbulent flow.

Even with the above simplifications one should appreciate the fact that the transient heat transfer problem between the heating fluid and the vehicle skin and between the vehicle skin and the outer flow are strongly coupled to one another. The derivation of the partial differential equations which describe this coupling is given in Section 2 of this report along with the various approximations which make the solution of these equations tractable. In Section 3, these equations are expressed in finite difference form so that the wall and heating fluid temperatures can be computed during the recovery period using numerical techniques.

Results from the numerical calculations are presented in Section 4 for several different scenarios whereby laminar flow may be lost. These scenarios include: the encounter with a turbulent "patch" embedded in the ambient fluid; the "sticking" of a particle originally suspended in the free stream to the vehicle surface for a short period of time (thus "tripping" the boundary layer); and the entry of a particle into the boundary layer and causing a localized turbulent "burst" which is then advected along the vehicle surface. The vehicle parameters selected in order to complete the numerical calculations (i.e., free-stream speed, body length, skin thickness and composition, and heating water flow rate and initial overheat) were based on the characteristics of a class of present-day tow-tank models. Since no particular vehicle is exactly modeled and because of the simplifications inherent with the present modeling, a one-to-one comparison between the measured gross operating conditions and those computed from the present model (such as the total heat transferred or the transition point location) would probably not be meaningful. The laminar flow recovery times should, however, be in the same neighborhood as might have been observed.

A discussion of the numerical results (for relatively short times into the recovery process) is also contained in Section 4. This is followed by an approximate, long-time analytical solution for the laminar flow recovery. This latter solution, when combined with the numerical results allows an estimation of the eventual recovery time.

Finally, conclusions and recommendations for future study are presented in Section 5 based on the findings contained herein.

2. FORMULATION OF COUPLED HEAT TRANSFER PROBLEM

As indicated earler, the heated vehicle is modeled as a flat plate configuration as shown in the following sketch:

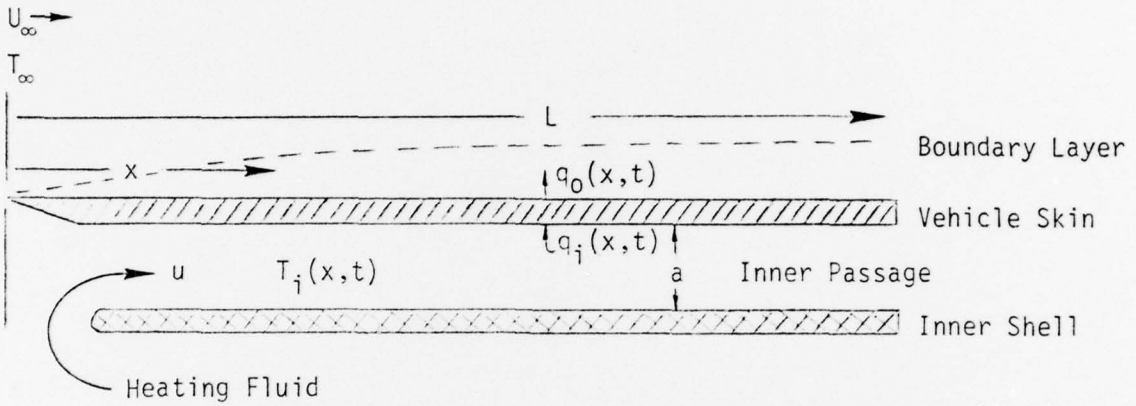

The vehicle is assumed to travel at speed U_∞ in water whose temperature is T_∞. Heating fluid (also assumed to be water) is introduced into the inner passage at the leading edge at temperature T_{i_0}. The inner shell is assumed to be an insulator. Heat is transferred from the fluid in the inner passage to the vehicle skin at a rate $q_i(x,t)$ and is removed from the vehicle skin by the external flow at a rate $q_o(x,t)$. The configuration is, in effect, a co-flow heat exchanger. The vehicle skin locally undergoes transient heating or cooling according to whether q_i is greater than or less than q_o. The detailed formulation of the analysis thus involves the coupled consideration of the inner flow passage, the vehicle skin and the external flow.

2.1 Inner Passage

The inner passage is assumed to be of constant cross-sectional height so that the mass flow per unit area is also constant. The flow in the inner passage is assumed to be a fully-developed turbulent flow of a constant property fluid. All extensive quantities associated with the heating water are per unit span.

Continuity considerations dictate that the mass flow per unit span, $m = \rho u a$, is constant. However, since the passage height, a, and fluid density, ρ, are each constant, the flow speed, u, is also constant. The momentum equation simply allows calculation of the pressure drop in the inner passage and is not of direct concern to the coupled heat transfer problem.

The equation for the fluid temperature in the inner passage, $T_i(x,t)$, is

$$\rho a c_i \frac{\partial T_i(x,t)}{\partial t} + \rho u a c_i \frac{\partial T_i(x,t)}{\partial x} = - q_i(x,t)$$

where c_i is the specific heat of the heating water and q_i is the heat flux from the heating fluid to the vehicle outer surface. Using the traditional approximation for the heat flux, this equation is written as:

$$\frac{\partial T_i}{\partial t} + u \frac{\partial T_i}{\partial x} = - \frac{h_i}{\rho a c_i} \left[T_i(x,t) - T_{w_i}(x,t) \right] \qquad (2.1)$$

where $T_{w_i}(x,t)$ is the temperature of the inner surface of the vehicle skin and h_i is the turbulent heat transfer coefficient for the flow in the inner passage. The heat transfer coefficient h_i can be obtained using Reynolds' analogy (see Reference 3);

$$h_i = \rho u c_i \frac{f}{8} Pr^{-2/3} \quad , \tag{2.2}$$

where the friction factor f is a function of the Reynolds number based on the hydraulic diameter of the inner passage and is evaluated from information on flow in circular pipes and Pr is the Prandtl number of the heating fluid.

Vehicle Skin

The relevant equation for the vehicle skin temperature, $T_w(x,t)$, is the transient energy equation

$$Mc_w \frac{\partial T_w(x,t)}{\partial t} = q_i(x,t) - q_o(x,t) \tag{2.3}$$

In this equation, Mc_w is the heat capacity of the vehicle skin per unit area, T_w is that skin temperature which best represents the heat content of the skin and is described in more detail below, and q_o is the heat flux to the outer flow from the wall. Because the vehicle skin thickness is small compared to length scales in the streamwise direction, we have ignored heat conduction along the vehicle in comparison to conduction through the skin.

Consider the skin to be a composite of a metal with a thin outer ceramic cladding, as shown in the sketch below. The rationale for selecting a composite skin is described in the Introduction. The overall thickness is ℓ.

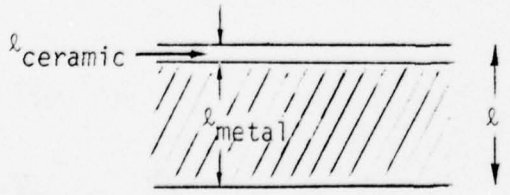

The heat capacity per unit area is then

$$Mc_w = (\rho c \ell)_{metal} + (\rho c \ell)_{ceramic} \qquad (2.4)$$

where here ρ is the density of the material under consideration and c is its specific heat. For such a composite, the thermal resistance, k, is the sum of the thermal resistances of each of the two layers.

The <u>effective</u> thermal conductivity of the composite is

$$k_{eff} = \frac{\ell}{\left(\frac{\ell}{k}\right)_{metal} + \left(\frac{\ell}{k}\right)_{ceramic}} = \frac{\ell}{\left(\frac{\ell}{k}\right)_{total}} \qquad (2.5)$$

If the base metal is, say, copper then the metal will dominate the heat capacity of the composite, while the ceramic coating would provide most of the resistance to heat transfer.

For computational purposes, it is easier to work with a skin of thickness ℓ having a constant k_{eff} as given by equation (2.5). In such an equivalent skin, the effective metal-ceramic interface is located according to their respective thermal resistances as shown in the sketch below:

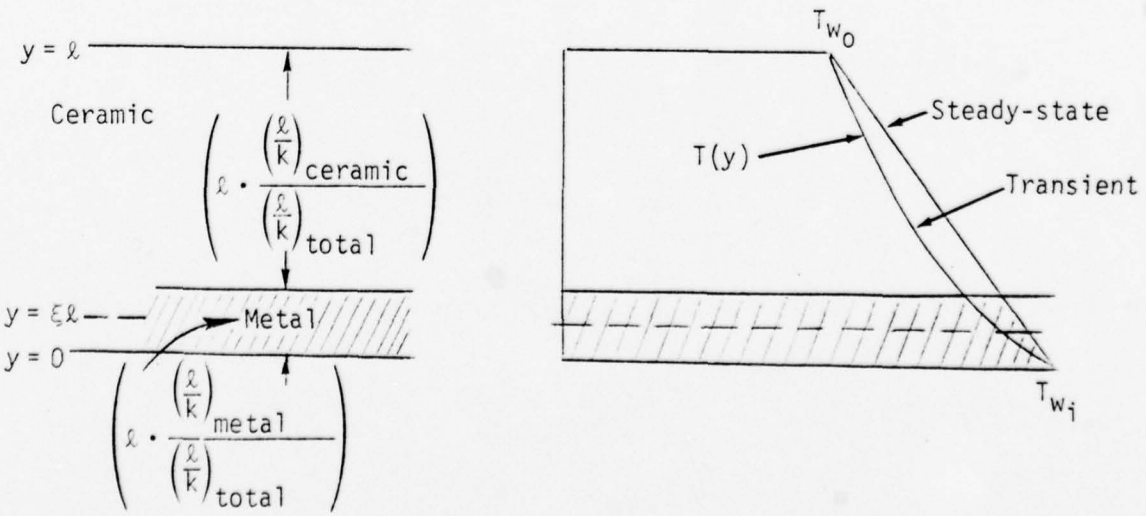

In a steady-state condition ($q_i = q_o$) the temperature decreases linearly in the stretched coordinate system as indicated in the sketch. For heat capacity purposes, the temperature T_w should be evaluated at or near the center of the metal layer, $y = \xi\ell$, where

$$\xi = \frac{1}{2} \frac{\left(\frac{\ell}{k}\right)_{metal}}{\left(\frac{\ell}{k}\right)_{total}} \quad . \tag{2.6}$$

In a transient situation ($q_i \neq q_o$), the temperature gradient is not constant even in a material of constant k_{eff}. As a first approximation, the temperature distribution through the skin will be assumed to be quadratic in the y-stretched coordinate system as indicated in the previous sketch.

The transient heat transfer rates into and out of the vehicle skin can be computed from Fourier's law of heat conduction as:

$$q_i(x,t) = - k_{eff} \left(\frac{\partial T}{\partial y}\right)_{y=0} \tag{2.7}$$

$$q_o(x,t) = - k_{eff} \left(\frac{\partial T}{\partial y}\right)_{y=\ell} \tag{2.8}$$

where $T(x,y,t)$ is the local, instantaneous temperature distribution in the equivalent skin with constant effective thermal conductivity.

2.2 Outer Flow

The heat removal rate $q_o(x,t)$ can also be written as

$$q_o(x,t) = h_o \left[T_{w_o}(x,t) - T_\infty\right] \tag{2.9}$$

where h_o is assumed to be the local flat-plate heat transfer coefficient. For a laminar boundary layer (see Reference 2)

$$(h_o)_{lam} = 0.332\ k\ Pr^{1/3} \sqrt{\frac{U}{\nu_\infty x}} = 0.332\ k\ Pr^{1/3} \sqrt{\frac{U}{\nu_\infty L}}\ \frac{x}{L}^{-1/2}$$

$$\equiv C_\ell \left(\frac{x}{L}\right)^{-1/2} \qquad (2.10)$$

while for a turbulent boundary layer (Reference 3)

$$(h_o)_{turb} = 0.0296\ k\ Pr^{1/3}\ \left(\frac{U}{\nu_\infty}\right)^{0.8} x^{-0.2} = 0.0296\ k\ \frac{Pr^{1/3}}{L^{0.2}} \left(\frac{U}{\nu_\infty}\right)^{0.8} \left(\frac{x}{L}\right)^{-0.2}$$

$$\equiv C_t \left(\frac{x}{L}\right)^{-0.2} . \qquad (2.11)$$

The boundary layer flow will be taken as laminar upstream of the transition point and turbulent downstream of the transition point. Except where turbulent flow is imposed (say by encountering a turbulent patch in the freestream) the transition Reynolds number for the flat-plate boundary layer will be assumed to be a function of $(T_{w_o} - T_\infty)$ only and the calculations by Wazzan *et al.* (Reference 4) which are based on the e^9 boundary-layer transition criterion will be used to approximate that functional dependence.

3. NUMERICAL METHOD FOR SOLVING THE COUPLED EQUATIONS

As developed in Section 2, the transient coupled equations for the heating fluid and vehicle skin are:

$$\frac{\partial T_i}{\partial t} + u \frac{\partial T_i}{\partial x} = - \frac{q_i(x,t)}{\rho a c_i} \tag{3.1}$$

$$\frac{\partial T_w}{\partial t} = \frac{q_i(x,t) - q_o(x,t)}{M c_w} \tag{3.2}$$

where the heat fluxes are

$$q_i = h_i \left[T_i - T_{wi} \right] \tag{3.3}$$

$$q_o = h_o \left[T_{wo} - T_\infty \right] \tag{3.4}$$

and the transition location between laminar and turbulent flow states is determined from the approximation shown in Figure 3.1 (page 17).

The temperature distribution across the vehicle skin is assumed quadratic at any instant and for all axial locations x so that

$$T(x,y,t) = a_o(x,t) + a_1(x,t)\, y + a_2(x,t)\, y^2 \tag{3.5}$$

with boundary conditions

$$\begin{aligned} T(x,0,t) &= T_{w_i}(x,t) \\ T(x,\ell,t) &= T_{w_o}(x,t) \quad . \end{aligned} \tag{3.6}$$

The coefficients a_o, a_1 and a_2 can be obtained as follows, since $T(x,\xi\ell,t) \equiv T_w$;

$$a_o = T_{wi}$$

$$a_1 = \frac{\xi^2 T_{wo} - (\xi^2-1)\, T_{wi} - T_w}{\xi \ell\, (\xi-1)} \tag{3.7}$$

$$a_2 = \frac{T_w - \xi T_{wo} + T_{wi}(\xi-1)}{\xi \ell^2 (\xi-1)}$$

The expressions for the heat flux into and out of the skin are therefore

$$q_i = - k_{eff} \left.\frac{\partial T}{\partial y}\right|_{y=0} = - \frac{k_{eff}}{\ell} \left[\frac{\xi^2 T_{wo} - (\xi^2-1) T_{wi} - T_w}{\xi\,(\xi-1)} \right] \tag{3.8}$$

$$q_o = - k_{eff} \left.\frac{\partial T}{\partial y}\right|_{y=\ell} = - \frac{k_{eff}}{\ell} \left[\frac{\xi(\xi-2) T_{wo} - (\xi-1)^2 T_{wi} + T_w}{\xi\,(\xi-1)} \right] \tag{3.9}$$

These expressions can be rewritten as

$$q_i = \beta_1 T_{wo} + \beta_2 T_{wi} + \beta_3 T_w \tag{3.10}$$

$$q_o = \alpha_1 T_{wo} + \alpha_2 T_{wi} + \alpha_3 T_w \tag{3.11}$$

where

$$\beta_1 = - \frac{k_{eff}}{\ell} \frac{\xi}{(\xi-1)} \quad ; \quad \alpha_1 = - \frac{k_{eff}}{\ell} \frac{(\xi-2)}{(\xi-1)}$$

$$\beta_2 = \frac{k_{eff}}{\ell} \frac{(\xi+1)}{\xi} \quad ; \quad \alpha_2 = \frac{k_{eff}}{\ell} \frac{(\xi-1)}{\xi}$$

$$\beta_3 = \frac{k_{eff}}{\ell} \frac{1}{\xi(\xi-1)} \quad ; \quad \alpha_3 = - \frac{k_{eff}}{\ell} \frac{1}{\xi(\xi-1)} .$$

Note that $\alpha_1 + \alpha_2 + \alpha_3 = 0$ and $\beta_1 + \beta_2 + \beta_3 = 0$.

Let $\Delta T_w = T_w - T_\infty$, $\Delta T_i = T_i - T_\infty$, $\Delta T_{wo} = T_{wo} - T_\infty$ and $\Delta T_{wi} = T_{wi} - T_\infty$. Then, by equating equations (3.10) and (3.11) with equations (3.3) and (3.4), we have

$$\beta_1 \Delta T_{wo} + (\beta_2 + h_i) \Delta T_{wi} = h_i \Delta T_i - \beta_3 \Delta T_w \tag{3.12}$$

$$(\alpha_1 - h_o) \Delta T_{wo} + \alpha_2 \Delta T_{wi} = - \alpha_3 \Delta T_w . \tag{3.13}$$

The solution of equations (3.12) and (3.13) for T_{wi} and T_{wo} is

$$T_{wi} = \frac{(\alpha_1 - h_o) h_i \Delta T_i + \left[\alpha_3 \beta_1 - \beta_3 (\alpha_1 - h_o)\right] \Delta T_w}{(\alpha_1 - h_o)(\beta_2 + h_i) - \alpha_2 \beta_1}$$

$$\equiv g_1 \Delta T_i + g_2 \Delta T_w \tag{3.14}$$

$$T_{wo} = \frac{-\alpha_2 h_i \Delta T_i + \left[\alpha_2 \beta_3 - \alpha_3 (\beta_2 + h_i)\right] \Delta T_w}{(\alpha_1 - h_o)(\beta_2 + h_i) - \alpha_2 \beta_1}$$

$$\equiv g_3 \Delta T_i + g_4 \Delta T_w \tag{3.15}$$

where

$$g_1 \equiv (\alpha_1 - h_o) h_i / E \tag{3.16}$$

$$g_2 \equiv \left[\alpha_3 \beta_1 - \beta_3 (\alpha_1 - h_o)\right] / E \tag{3.17}$$

$$g_3 \equiv - \alpha_2 h_{i/E} \tag{3.18}$$

$$g_4 \equiv \left[\alpha_2 \beta_3 - \alpha_3 (\beta_2 + h_i)\right] / E \tag{3.19}$$

and

$$E \equiv (\alpha_1 - h_o)(\beta_2 + h_i) - \alpha_2\beta_1 \ . \tag{3.20}$$

The coupled partial differential equations (1) and (2) for the dependent quantities T_i and T_w can be then rewritten as

$$\frac{\partial \Delta T_i}{\partial t} + \frac{u}{L}\,\frac{\partial(\Delta T_i)}{\partial(x/L)} = -\,\frac{h_i}{\rho a c_i}\,\left[(1-g_1)\,\Delta T_i - g_2\,\Delta T_w\right] \tag{3.21}$$

$$\frac{\partial \Delta T_w}{\partial t} = \frac{\left[h_i(1-g_1) - h_o g_3\right]\Delta T_i}{Mc_w} - \frac{\left[h_i g_2 + h_o g_4\right]\Delta T_w}{Mc_w} \tag{3.22}$$

where L is the overall length of the vehicle.

The heat transfer coefficients h_o and h_i are taken as

$$h_o = \begin{cases} c_\ell \left(\frac{x}{L}\right)^{-0.5} & \text{for laminar flow} \\ \\ c_t \left(\frac{x}{L}\right)^{-0.2} & \text{for turbulent flow} \end{cases} \tag{3.23}$$

and

$$h_i = \rho u c_i \left(\frac{f}{8}\right) Pr^{-2/3} \qquad \text{fully turbulent channel flow} \tag{3.24}$$

where the friction factor f is a function of the Reynolds number based on the hydraulic diameter of the inner passage and is evaluated from information on flow in circular pipes.

The transition Reynolds number versus the required (constant) wall temperature overheat for a flat plate can be plotted as shown in Figure 3.1. For computational purposes, this curve is fit approximately by the fifth-degree polynomial

$$(\Delta T)_{tr} \doteq c_o + c_1 \left(\frac{Re_{tr}}{10^6}\right) + c_2 \left(\frac{Re_{tr}}{10^6}\right)^2 + \ldots c_5 \left(\frac{Re_{tr}}{10^6}\right)^5 \qquad (3.25)$$

where $Re_{tr} = \dfrac{ux_{tr}}{\nu_\infty}$ and

$$c_o = -4.31002$$

$$c_1 = 1.29390$$

$$c_2 = -2.78416 \times 10^{-2}$$

$$c_3 = 3.70249 \times 10^{-4}$$

$$c_4 = -2.52094 \times 10^{-6}$$

$$c_5 = 6.91835 \times 10^{-9}$$

By comparing the wall overheat temperature ΔT_{wo} determined from equation (3.15) (using solutions for ΔT_i and ΔT_w), and the transition criterion of equation (3.25), one can determine the regimes of laminar or turbulent flow. Note that this procedure ignores the influence of the upstream wall temperature variations since comparisons are made locally with a transition criterion based on an assumed uniform and steady wall temperature. To incorporate the spatial and temporal changes of the upstream wall temperature into a transition criterion would be so complicated and time consuming that it would overwhelm all other considerations. In effect, a

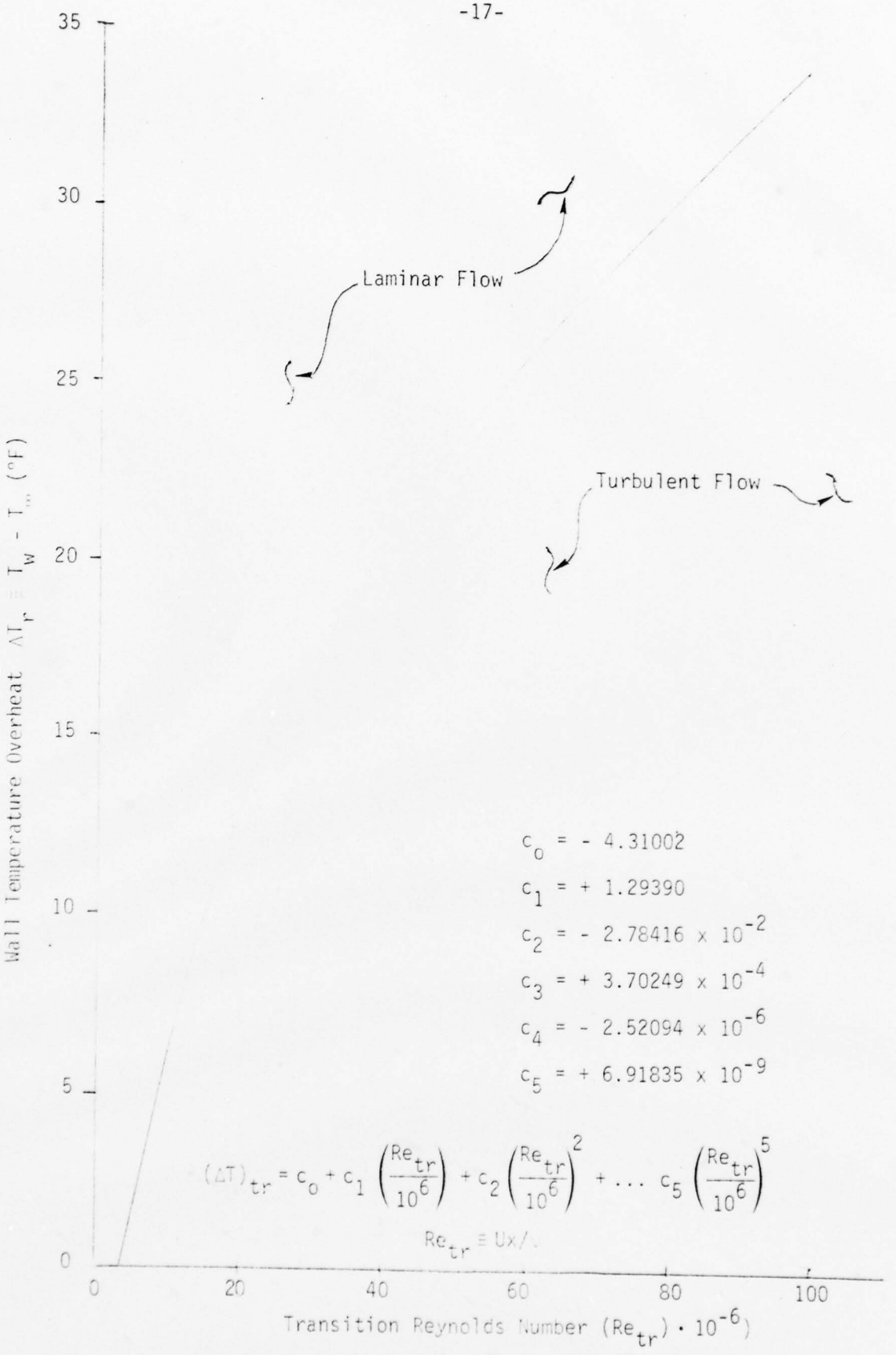

Figure 3.1. Wall Temperature Overheat Versus Transition Reynolds Number for a Flat Plate

complete boundary-layer stability calculation would be required at each time step during the recovery period. It was the authors' belief that the above simple criterion would provide reasonably accurate estimates of the transition point throughout the recovery period (at least to within the order of accuracy of other assumptions made).

3.1 Steady Flow Conditions

When a stead-state condition is achieved, equations (3.21) and (3.22) may be combined into a single ordinary differential equation whose closed-form solution can be derived once the heat transfer coefficients h_i and h_o are specified. For computational reasons, however, it was more expeditious to formulate the separate equations in finite-difference format and solve the equations numerically. This allowed initial conditions for the transient solutions to be calculated directly (and with similar algorithms) rather than having to be computed from the (complicated) closed-form solution. It should be added that the numerical and analytical solutions agreed with one another quite closely. The steady-state form of equations (3.21) and (3.22) are:

$$\frac{\partial(\Delta T_i)}{\partial(x/L)} = - \frac{h_i}{\rho a c_i} \frac{L}{u} \left[(1-g_1)\Delta T_i - g_2 \Delta T_w\right] \tag{3.26}$$

$$\Delta T_w = \frac{h_i(1-g_1) - h_o g_3}{h_i g_2 + h_o g_4} \Delta T_i \quad . \tag{3.27}$$

Equations (3.26) and (3.27), when written in finite difference form, become

$$(\Delta T_i)_{j+1} = (\Delta T_i)_j - \Delta(x/L) \frac{h_i L}{\rho a c_i u} \left[(1-g_1)(\Delta T_i)_j - g_2 (\Delta T_w)_j\right] \tag{3.28}$$

$$(\Delta T_w)_j = \frac{h_i(1-g_1) - h_o g_3}{h_i g_2 + h_o g_4} (\Delta T_i)_j \tag{3.29}$$

The initial condition for ΔT_i is prescribed and the initial condition for ΔT_w is computed from the two companion relations

$$\Delta T_{wi}\Big|_{x=0} = \frac{h_i \, \Delta T_i}{(\beta_2 + h_i) + \beta_3(1-\xi)} \tag{3.30}$$

$$\Delta T_{wo}\Big|_{x=0} = 0 \tag{3.31}$$

in conjunction with equations (3.14) and (3.15).

3.2 Transient Conditions

For transient conditions, the finite difference equations for the heating fluid temperature and mean wall temperature are

$$(\Delta T_i)_j^{n+1} = (\Delta T_i)_j^n - \Delta t \left\{ \frac{u}{2\Delta(x/L)} \left[(\Delta T_i)_{j+1}^n - (\Delta T_i)_{j-1}^n \right] + \frac{h_i}{\rho a c_i} \left[(1-g_1)(\Delta T_i)_j^n - g_2 (\Delta T_w)_j^n \right] \right\} \tag{3.32}$$

$$(\Delta T_w)_j^{n+1} = (\Delta T_w)_j^n + \Delta t \left[\frac{h_i(1-g_1) - h_o g_3}{M c_w} (\Delta T_i)_j^n - \frac{h_i g_2 + h_o g_4}{M c_w} (\Delta T_w)_j^n \right]$$

where the superscript n denotes a value at the nth time step in the calculation and Δt is the time interval.

The initial conditions for these equations are identical to those mentioned in Section 3.1 at $x = 0$ and for $x > 0$ they are taken as the steady-state solution described in Section 3.1 (usually the laminar flow solution except for the case of an encounter with an infinitely long turbulent patch in which case the fully-turbulent, steady state temperature distribution was used).

3.3 Computer Program

A computer program based on an explicit finite-difference method was written to solve the coupled difference equations. The procedure used for each calculation is described below:

1. Input the data including initial flow state (laminar or turbulent).

2. Calculate the steady state temperature distributions from equations (3.28) and (3.29).

3. Calculate the transient temperatures by using the finite differenced equations (3.32) and (3.33).

4. Use the transition criterion (equation (3.25)) to determine the local flow condition (i.e., either laminar or turbulent external flow).

4. EXAMPLES AND DISCUSSION

In this study, four types of transient response scenarios are treated. They are:

1. Recovery from a long turbulent patch. In this case, the vehicle is assumed to have been exposed to fully turbulent flow for a long enough period to reach turbulent steady-state conditions.

   $t \leq 0$ steady turbulent external flow

   $t > 0$ transient recovery toward laminar external flow

2. Response to and recovery from an encounter with a finite length turbulent patch embedded in the free-stream.

   $t \leq 0$ steady laminar flow

   $-T_t < t \leq 0$ fully turbulent external flow for a time period of T_t (sec)

   $t > 0$ transient recovery toward laminar external flow

3. Response to and recovery from a temporary boundary layer trip at a fixed surface location

   $t \leq 0$ steady laminar flow

   $-T_t < t \leq 0$ and $x \geq x_t$ turbulent flow conditions for a time period of T_t (sec) downstream of X_t (ft)

   $t > 0$ transient recovery toward laminar external flow

4. Recovery from a turbulent spot generated at location x_t within the laminar boundary layer. This spot is then swept by the flow along the flat-plate surface according to the sketch shown below.

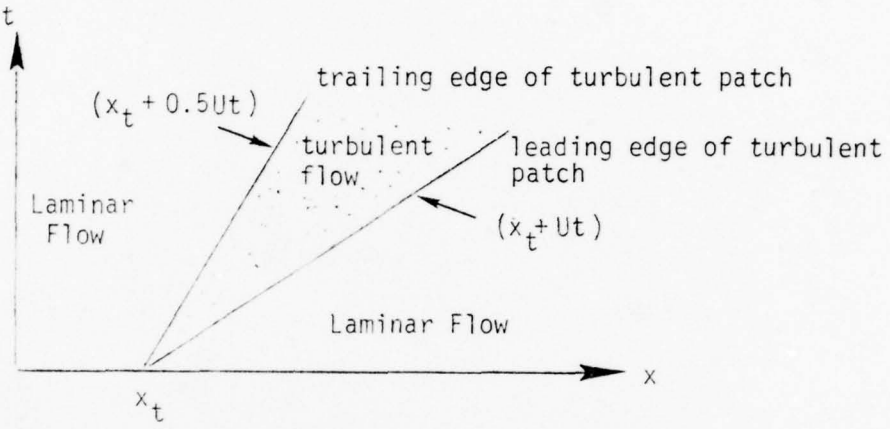

These "turbulent spots" are, of course, assumed to be two-dimensional in the present context.

4.1 Configuration Parameters

The flat-plate is assumed to have a length, L = 12.45 ft. The skin composition, which is believed to be representative of present-day experimental vehicles, is a 0.25" thick sheet of copper coated with 0.007" of a ceramic material. For this skin composition and using tabulated thermal properties for each material, such as are given in Reference 5, it may be shown that:

$$\frac{k_{eff}}{\ell} = 0.495 \ \frac{Btu}{sec\text{-}ft^2\text{-}^oF}$$

$$Mc_w = 1.084 \ \frac{Btu}{ft^2\ ^oF}$$

$$\xi = 0.0844$$

The heating water is assumed to have a flow speed of 1.53 ft/sec in a channel 0.01 ft thick. This corresponds to a flow rate of 0.96 lb_m/sec per foot of span width which is also believed representative of present day experimental vehicle flow rates.

4.2 Steady State Solutions

For each choice of operating conditions (free-stream speed, heating water flow rate and inlet temperature) the steady state temperature distributions along the length of the flat plate were computed. The results for a typical case (U = 20 knots, $T_\infty = 70^oF$, $(\Delta T_i)_o = 55^oF$) are shown in Figure 4.1. Note that the outside wall temperatures, both laminar and turbulent, rise abruptly from the leading edge (where the temperature must equal the free-stream fluid temperature) to a maximum value at between 10% and 30% of the flat plate length and decrease slowly thereafter. Note, however, the large differences in level between the two cases. In order to properly maintain a steady laminar external flow, the outside wall temperature difference should everywhere exceed that prescribed by the e^9 transition criterion.

In the laminar situation the heating water loses 44% of its initial heat content while in the turbulent case, because of the higher heat transfer rate to the external flow, the heating water loses 78% of its initial heat content. At the trailing edge of the plate with fully laminar flow, the outside wall temperature exceeds that required to just maintain laminar flow by 3.0^oF. If the initial heating water temperature difference $(\Delta T_i)_o$ were to be reduced to 47.8^oF, the wall temperature excess at the trailing edge of the plate would be reduced to zero. It will be shown in Section 4.4 that the time required for laminar flow to be fully recovered after some turbulent event is a sensitive function of this temperature excess. When the wall temperature excess at the trailing edge is zero, the recovery time is infinite.

Figure 4.1 Steady State Temperature Distributions

U = 20 knots (33.8 ft/sec)

$T_\infty = 70^oF$ $(\Delta T_i)_o = 55^oF$

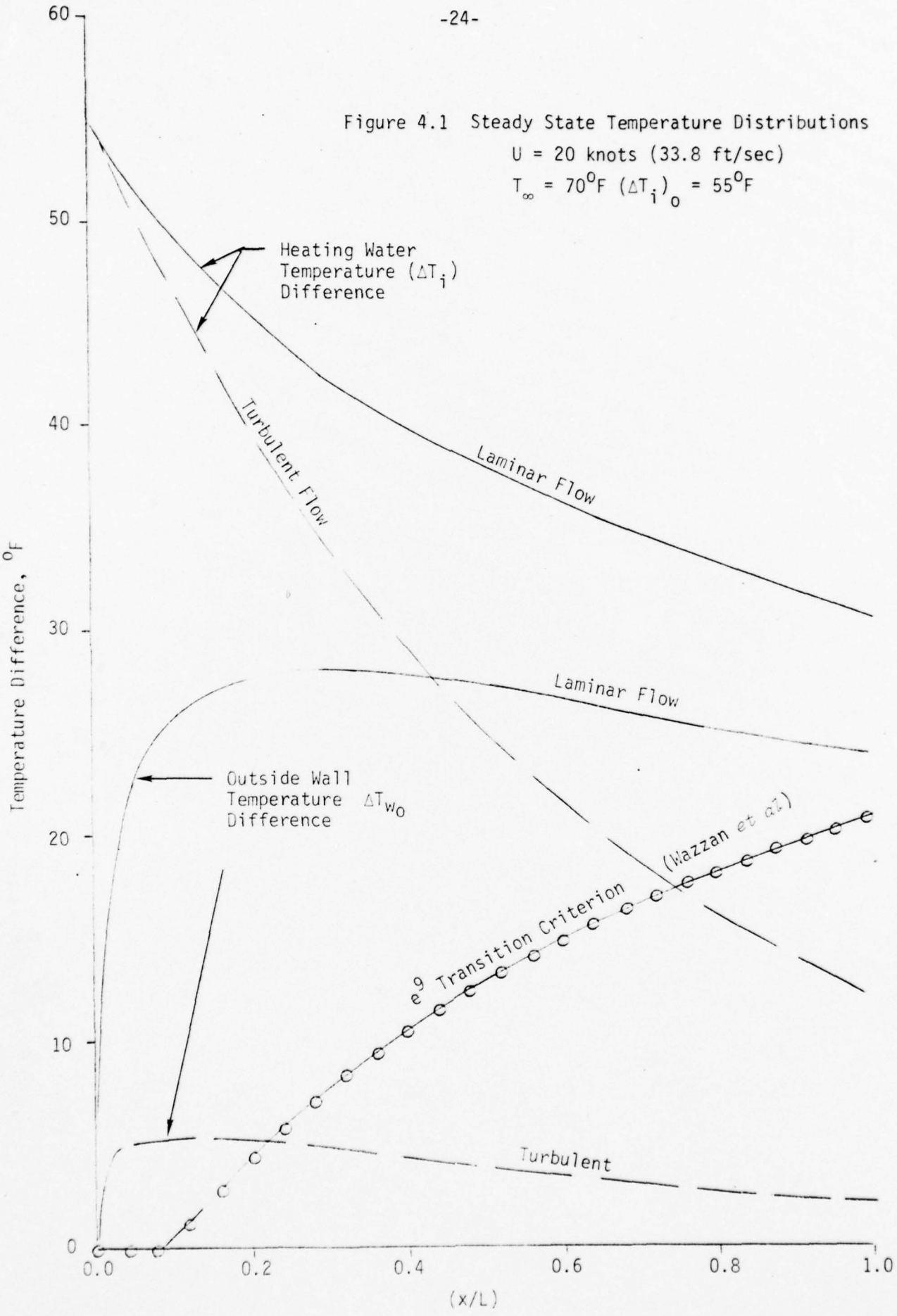

The results of the steady-state calculations for free-stream speeds of 20, 40 and 50 knots are summarized in Table 4.1. The changes of the laminar heat loss and the trailing edge wall temperature excess to changes in the initial heating water temperature (above the minimum required value) are shown in Table 4.2.

Table 4.1

RESULTS OF STEADY STATE SOLUTIONS

(L = 12.45 ft. $\dot{m}$ = 0.96 lb_m/sec - ft of width)

Free-Stream Speed (knots)	Heating Water Inlet Temp. (^oF above ambient) $(\Delta T_i)_o$	Heat Power at Inlet $\dot{m}(\Delta T_i)_o c$ kw/ft of width	Laminar Heat Power Loss kw/ft of width	Turbulent Heat Power Loss kw/ft of width	Trailing Edge Wall Temp. Excess ^oF
20	47.8	48.4	21.3	38.6	0
	55	55.7	24.7	43.6	3.0
	60	60.8			5.2
40	86	87.1	44.5	70.8	0
	90	91.2			1.4
	95	96.2			3.1
50	105	106.4	57.0	85.5	0
	115	116.5			3.2
	120	121.6			4.8

Table 4.2

SENSITIVITY TO HEATING WATER INLET TEMPERATURE DIFFERENCE

($L = 12.45$ ft. $m = 0.96$ lb_m/sec - ft of width)

Free-Stream Speed (knots)	Laminar Heat Flux Increment per unit Heating Water Temperature Increase kw/ft of width per ^oF	Trailing Edge Wall Temp. Excess per unit Heating Water Temp. Increase $^oF/^oF$
20	0.47	0.43
40	0.53	0.34
50	0.53	0.32

4.3 Results of Numerical Calculations

The results of the calculations for the various recovery scenarios will now be presented. The results will be shown only for about the first four seconds into the recovery history. The principal reason for this is that, for later times, the explicit finite-difference technique used to solve the coupled partial differential equations becomes unstable. This numerical instability manifests itself initially as small "wiggles" about the mean axial distribution after about 8 seconds into the recovery period and these wiggles become larger and larger at later times. This instability is a result of the numerical algorithm employed rather than being a result of the equations. Rather than attempting to incorporate a more sophisticated technique in order to extend the computations, we have instead found an approximate analytical solution which is valid for the latter stages of the recovery period. This analytical solution is described in Section 4.4 of the present report. The key to combining

the early-time numerical solution with the late-time analytical solution is that the latter requires an initial condition which is provided by the numerics at four seconds. Thus, the entire recovery process is describable and the matching between the early and late time solutions is not critically dependent on the precise matching time. The details of the matching procedure and estimates for the recovery time are also described in Section 4.4.

4.3.1. Recovery From "Long" Turbulent Patch

The initial wall and fluid temperatures used for the recovery calculations described in this section are taken as those corresponding to a fully-turbulent external boundary layer. This is the most "severe" deviation imaginable from a fully laminar external boundary layer and corresponds to the flat plate encountering a very long turbulent patch embedded in the ambient fluid. Three representative calculations are shown in Figures 4.2, 4.3 and 4.4 where the outside wall temperature histories are shown for several seconds after the flat-plate exits from the turbulent patch.

In Figure 4.2, for example, the steady-state laminar and turbulent flow wall temperature distributions are shown as well as the wall temperature distribution required to prevent natural boundary layer transition according to the e^9 criterion. The outside wall temperature distributions, ΔT_{w_o}, for several times after exit from a turbulent patch are shown.*

* The present calculations assume that at $t = 0$ the imposed external turbulent flow completely vanishes leaving only the natural transition to turbulent flow within the boundary layer rather than accounting for the fact that the turbulent patch's edge would move rearward along the plate at 33.8 ft/sec. The difference between these two is slight since the natural transition point moves so much slower than the free-stream speed (this was the case in every calculation).

Figure 4.2 Recovery From Steady-State Turbulent Flow

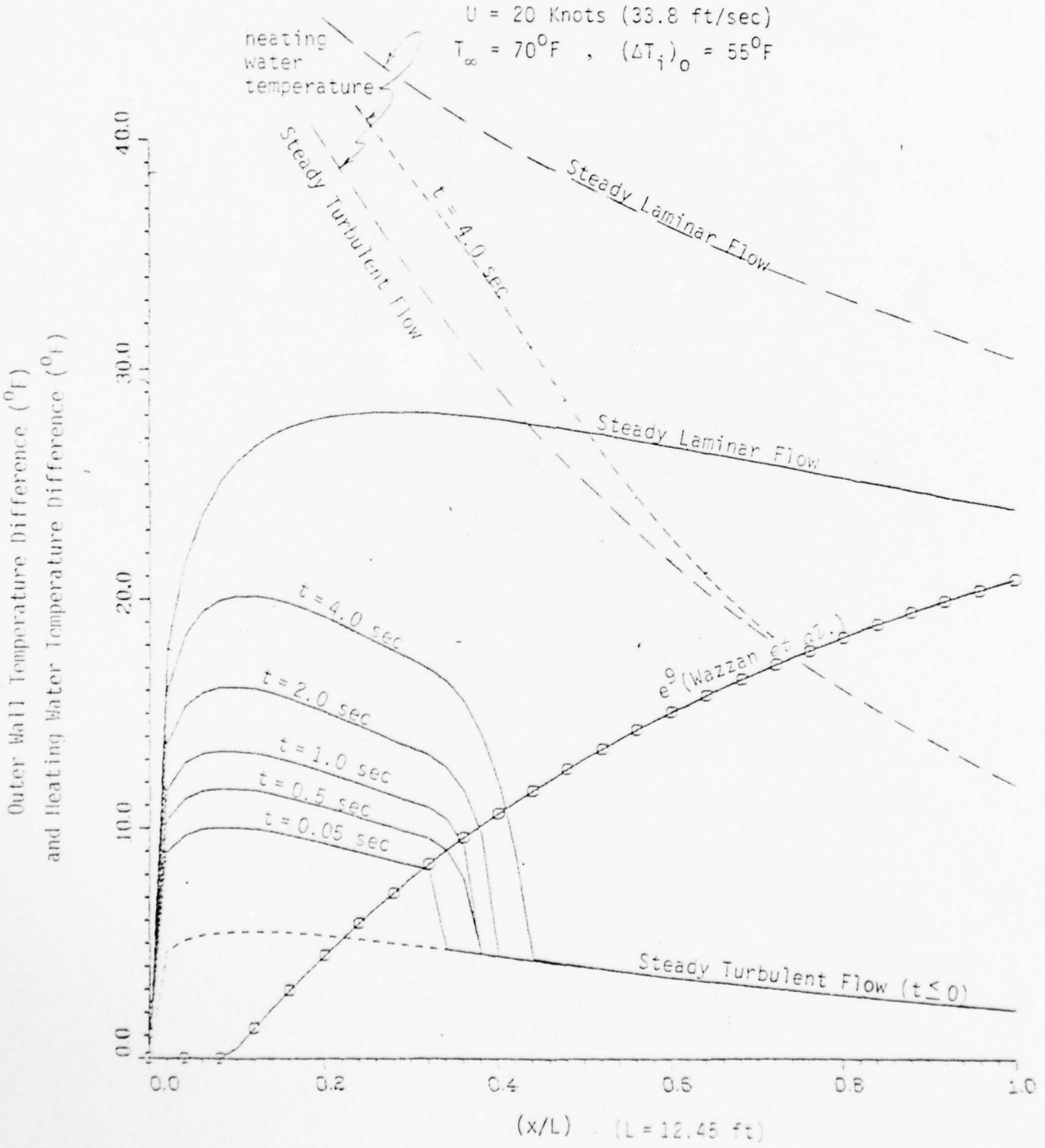

Figure 4.3. Recovery From Steady-State Turbulent Flow

$U = 20$ Knots (33.8 ft/sec)

$T_\infty = 70^\circ F$, $(\Delta T_i)_o = 60^\circ F$

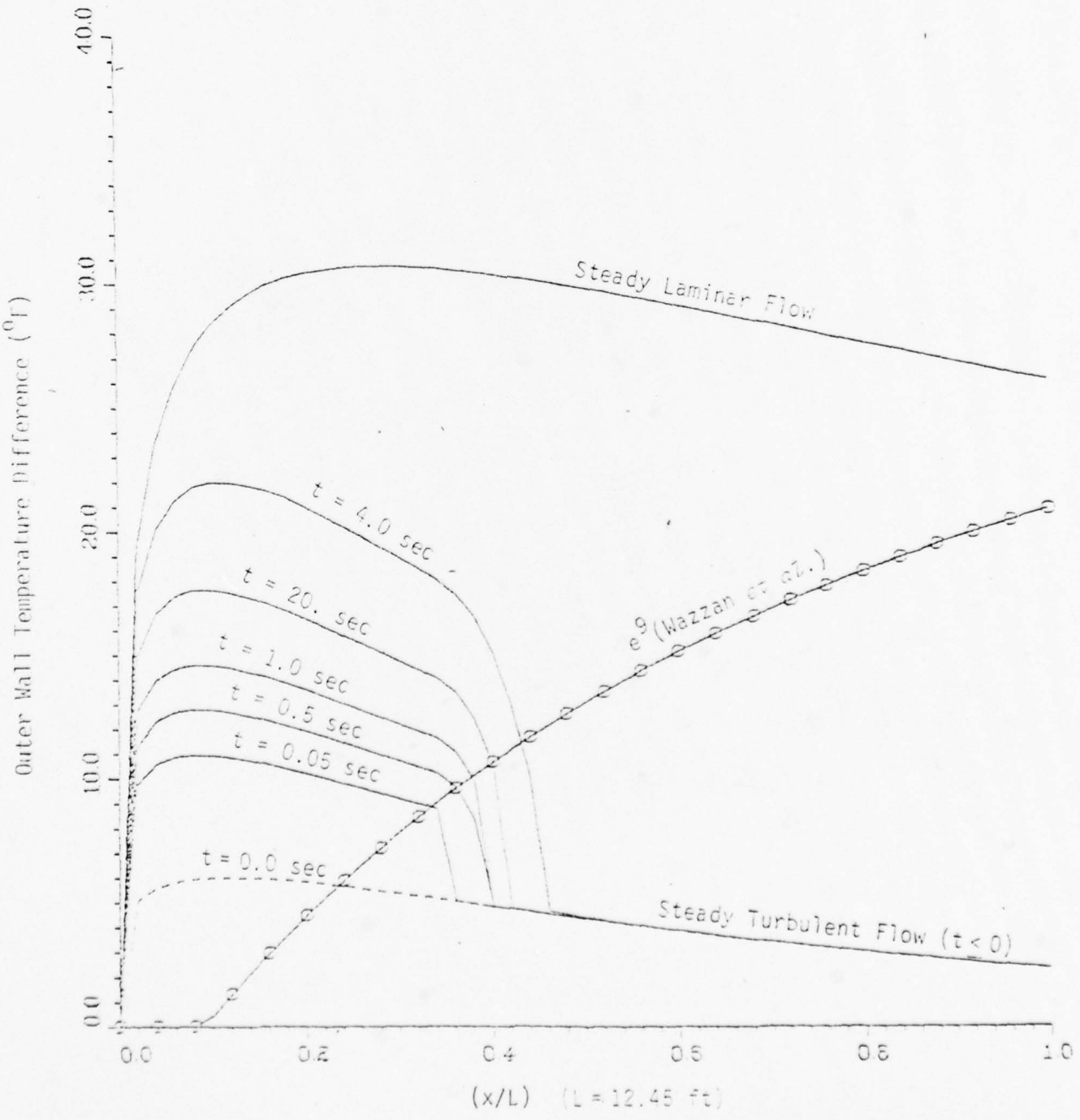

Figure 4.4. Recovery From Steady-State Turbulent Flow

U = 40 Knots (67.6 ft/sec)

$T_\infty = 70^oF$, $(\Delta T_i)_o = 95^oF$

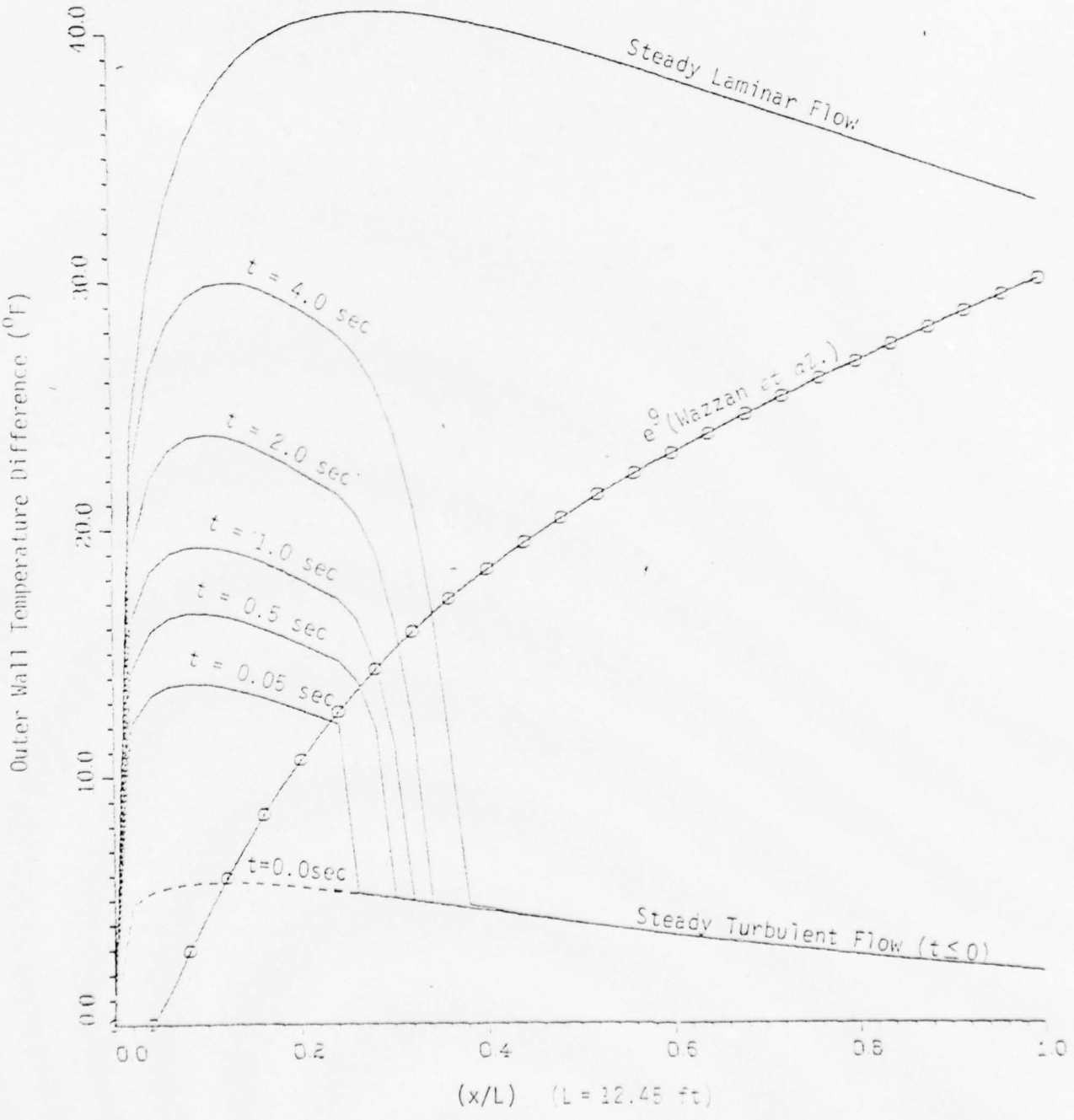

Note that after removal of the imposed external turbulent flow in Figure 4.2, the transition location virtually "jumps" to a location 30% aft of the leading edge and then progresses at a much slower rate toward the trailing edge (i.e., in the first 0.05 seconds, the transition location moves from $x/L \approx 0.2$ to $x/L \approx 0.3$ and nearly four seconds later the transition point has only progressed to $x/L \approx 0.4$). This characteristic "jump and creep" motion of the transition point has been observed in nearly every calculation. The heating water temperatures are also shown in Figure 4.2 (only) for the fully laminar, fully turbulent and for an intermediate time during recovery.

4.3.2 Recovery From Finite Length Turbulent Patch Encounter

If the flat-plate were to encounter a finite length turbulent patch embedded in the ambient water, the wall temperature, upon exiting the patch, would not be as depressed as in the previous case. Because of this, one might expect that the recovery time would be shorter than the case considered in Section 4.3.1. To demonstrate that this is indeed the situation, calculations for operating conditions similar to those considered previously were performed but for which the turbulent "soak time" was several seconds. The calculated outer wall temperature histories for two of these cases are shown in Figures 4.5 and 4.6. For both of these the turbulent patch length was taken as 67.6 feet (i.e., a duration of 2 seconds and 1 second for speeds of 20 knots and 40 knots, respectively). After exiting the turbulent patch, the natural boundary layer transition point is again seen to "jump" to an initial location and then to "creep" toward the flat-plate's trailing edge. Notice that downstream of the transition location, the wall temperature continues to decrease even after the turbulent patch is exited because the boundary layer is still turbulent there, and as long as it remains turbulent, it tends toward the level for steady turbulent flow. The eventual laminar flow recovery time for these (and other) cases will be discussed in Section 4.4.

Figure 4.5. Recovery From Encounter with Turbulent Patch

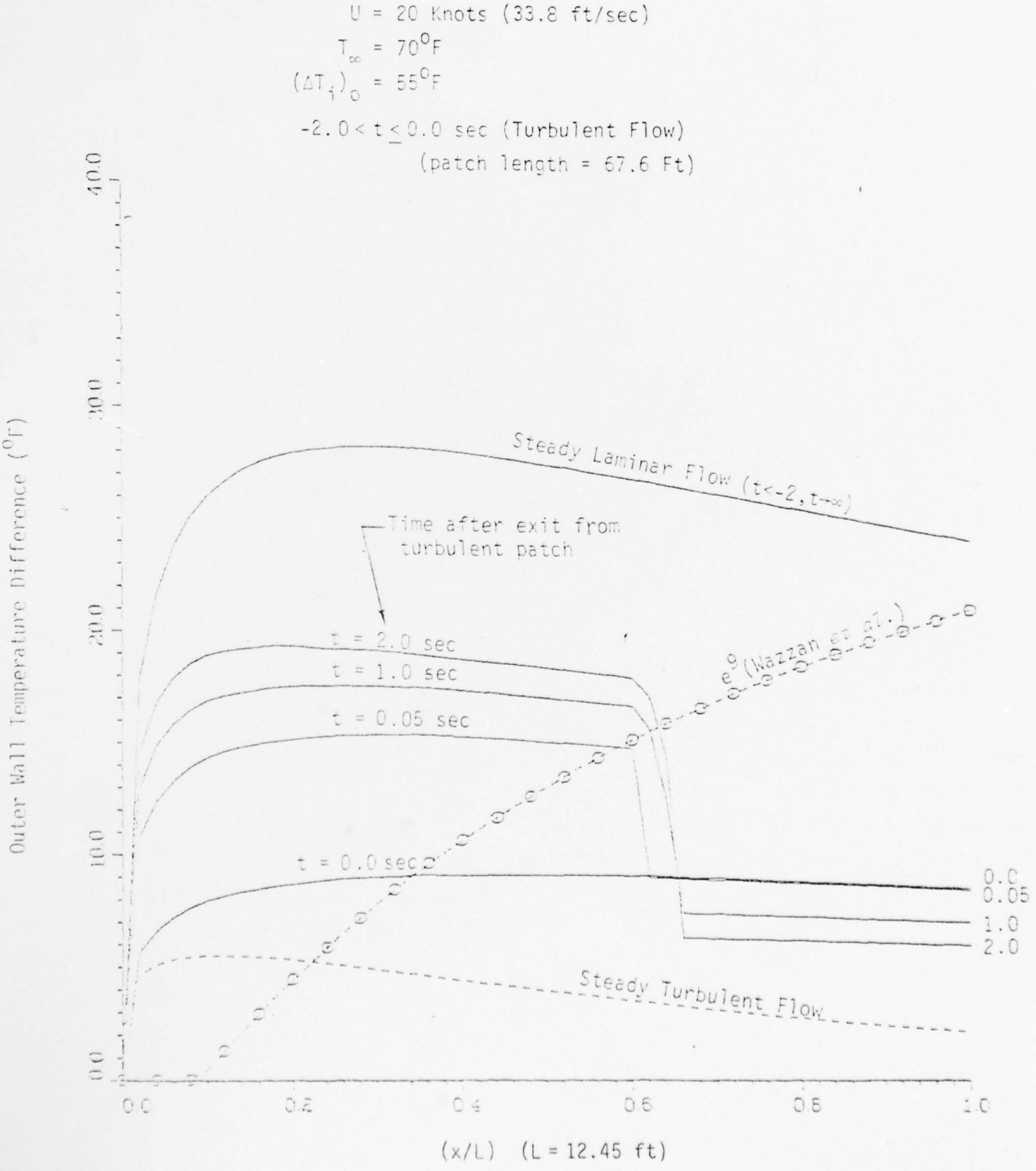

Figure 4.6. Recovery From Encounter with Turbulent Patch

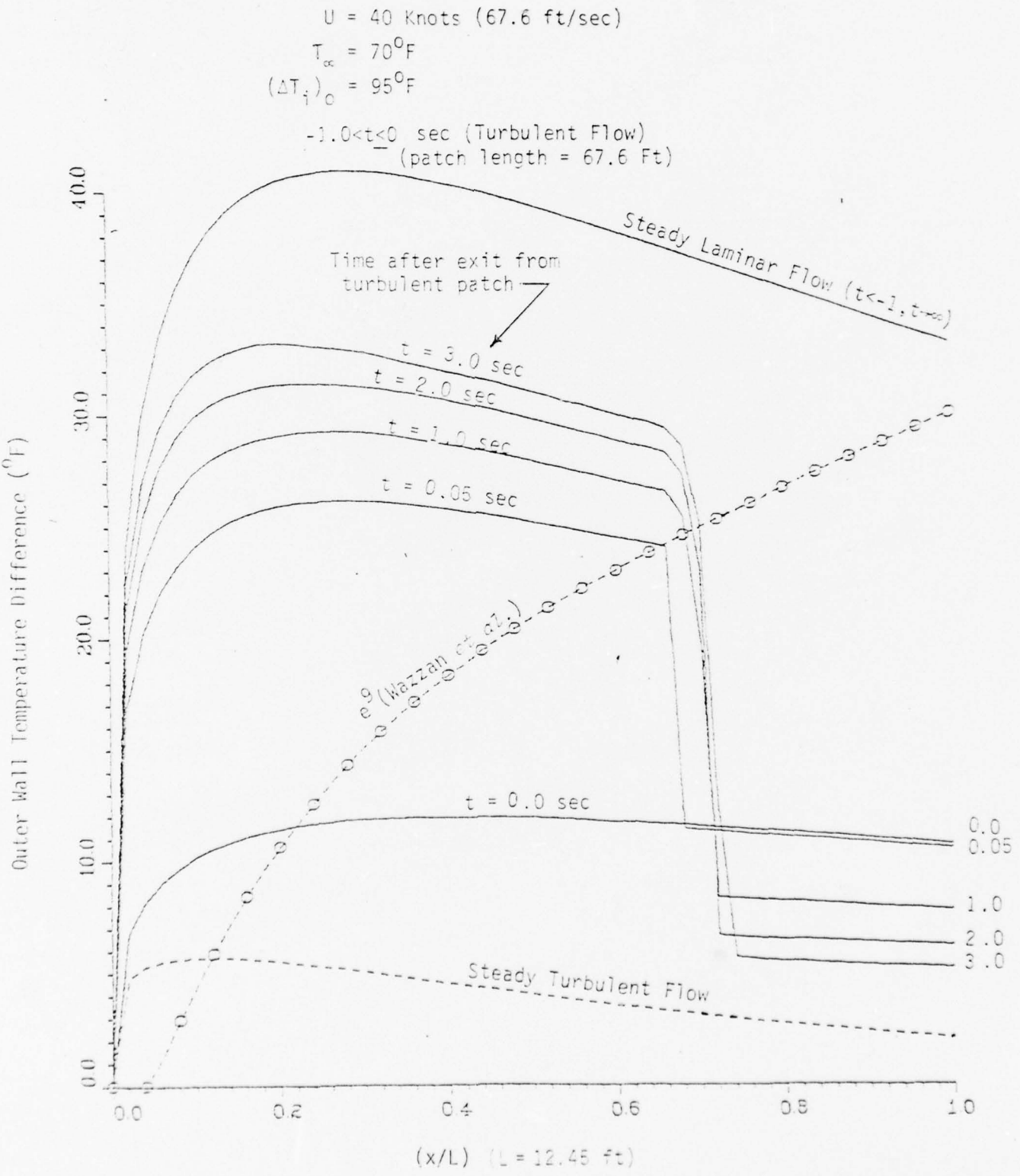

4.3.3 Recovery From a Particle Temporarily "Stuck" to the Vehicle Surface

One other situation whereby laminar flow could be lost is by the adherence of a solid particle (say, originally suspended in the ambient fluid) to the surface of the heated body which then "trips" the laminar boundary layer. This situation was also numerically modeled and some representative results are shown in Figures 4.7 and 4.8 for the same two operating conditions considered in the previous section. For these figures, it has been assumed that the particle adheres to the flat-plate surface two feet aft of the leading edge and that it remains stuck for a vehicle travel distance of 20.3 feet (0.6 sec. duration at 20 knots, 0.3 sec. at 40 knots). Because this particular case is less severe than the previous two cases, the natural transition point almost "jumps" past the plate's trailing edge once the particle is dislodged as may be seen in both Figures 4.7 and 4.8. After this initial jump, the previously described "creep" toward the trailing edge is also noted, however.

4.3.4 Recovery From a Turbulent Spot Created Within the Original Laminar Boundary Layer

The last laminar flow loss/recovery history computation is representative of the situation where a particle (originally suspended in the ambient fluid) enters the flat plate's laminar boundary layer and, in doing so, locally disrupts the flow field. In effect, a turbulent spot is created which is then swept by the flow along the length of the plate. The leading edge of the turbulent spot is assumed to be advected at the free-stream speed whereas its trailing edge is assumed to move downstream at one-half the freestream speed. Thus, the spot's extent grows as it is swept along the plate.

Calculations of such an occurrence are shown in Figures 4.9 and 4.10 again for the two nominal operating conditions considered. In either

Figure 4.7. Recovery From Temporary Boundary Layer Trip

U = 20 Knots (33.8 ft/sec)

$T_\infty = 70^oF$, $(\Delta T_i)_o = 55^oF$

$x \geq 2$ ft and $0.6 < t \leq 0$ sec } Turbulent Flow

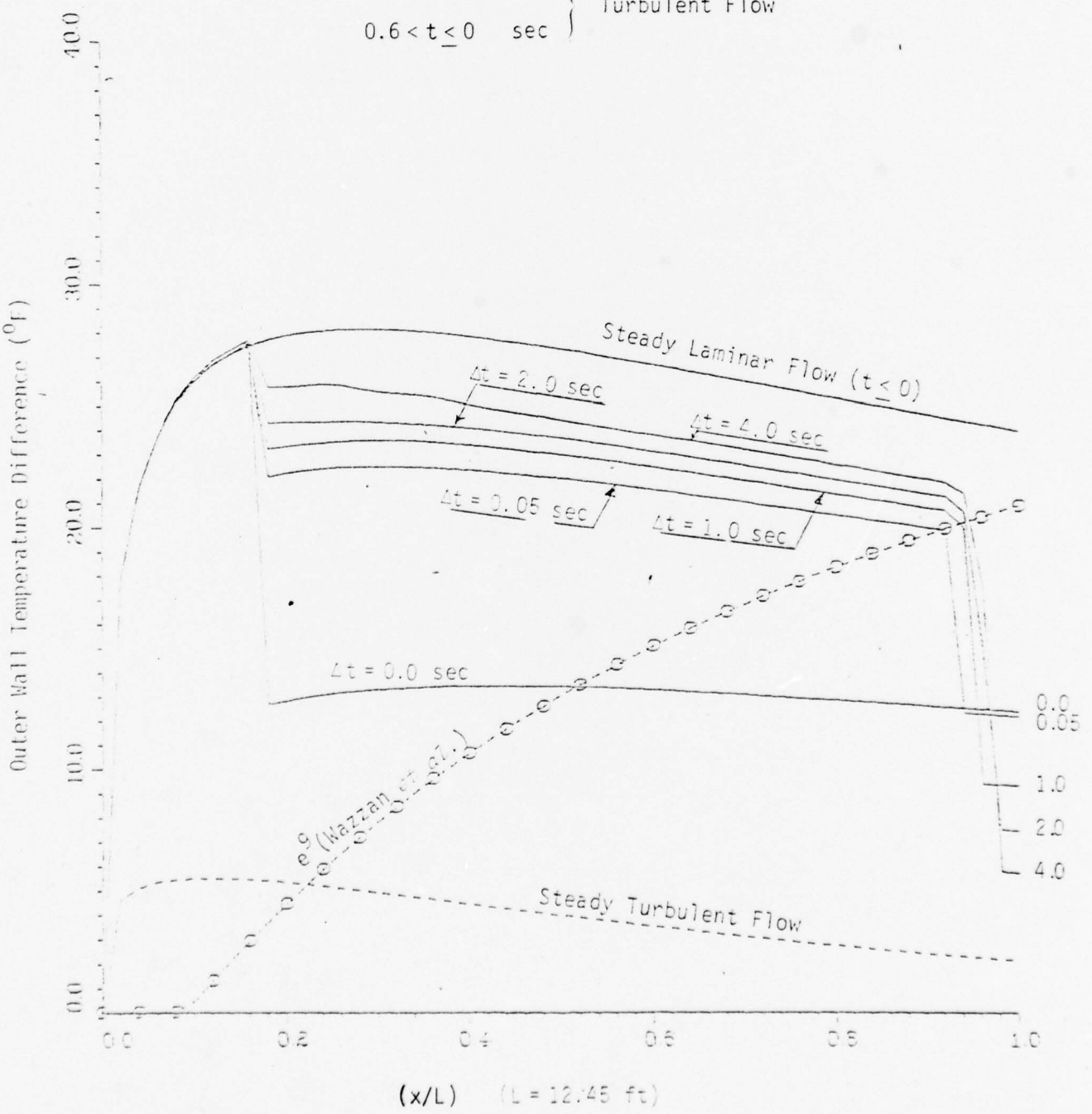

Figure 4.8 Recovery From Temporary Boundary Layer Trip

U = 40 Knots (67.6 ft/sec)

$T_\infty = 70^oF$, $(\Delta T_i)_o = 95^oF$

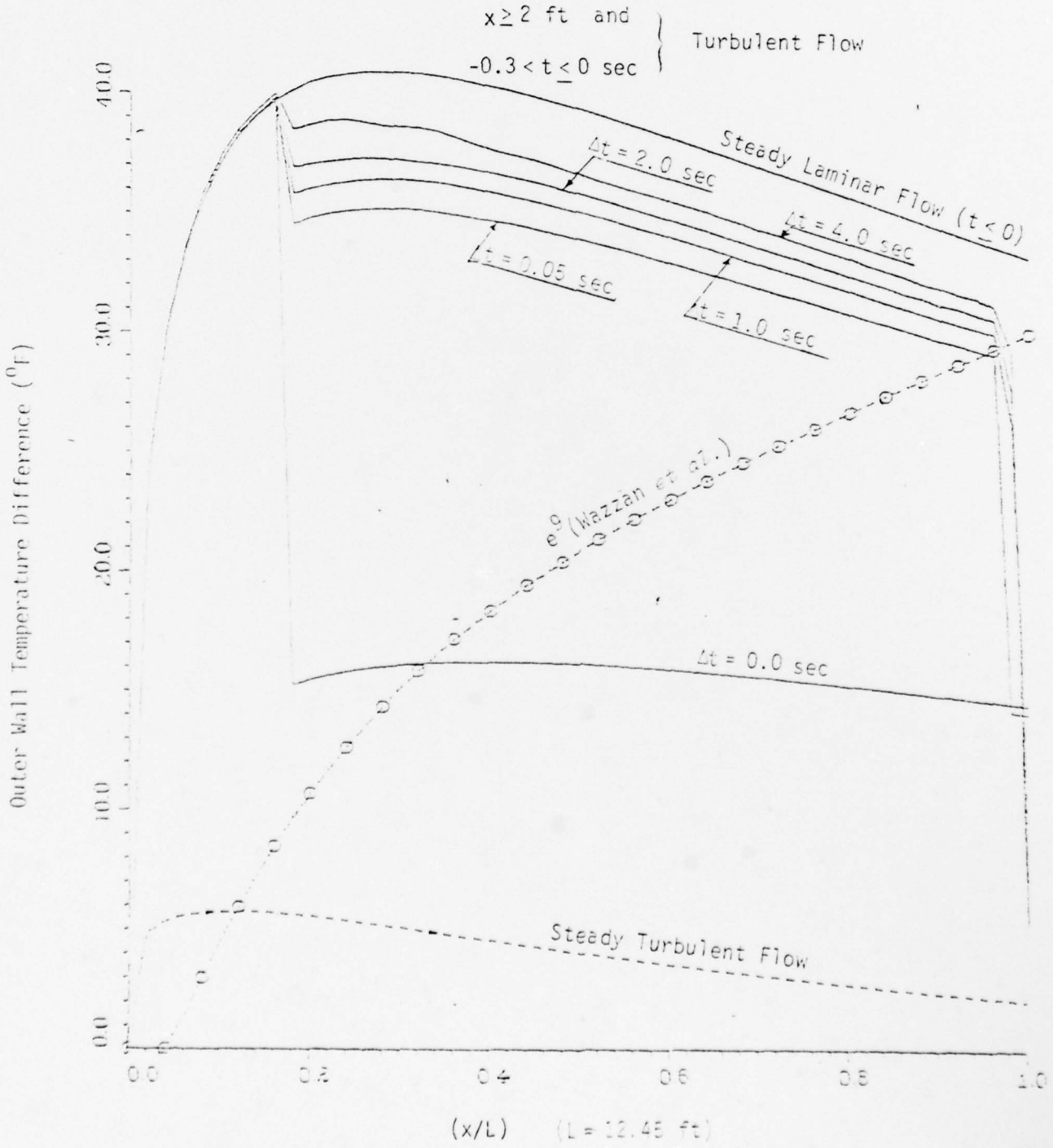

Figure 4.9 Recovery From a Single Turbulent Spot

$U = 20$ Knots (33.8 ft/sec)

$T_\infty = 70^oF$, $(\Delta T_i)_o = 55^oF$

$(x_t + 0.5\,Ut) \geq x \geq (x_t + Ut)$ Turbulent Flow

$x_t = 0.0$ ft.

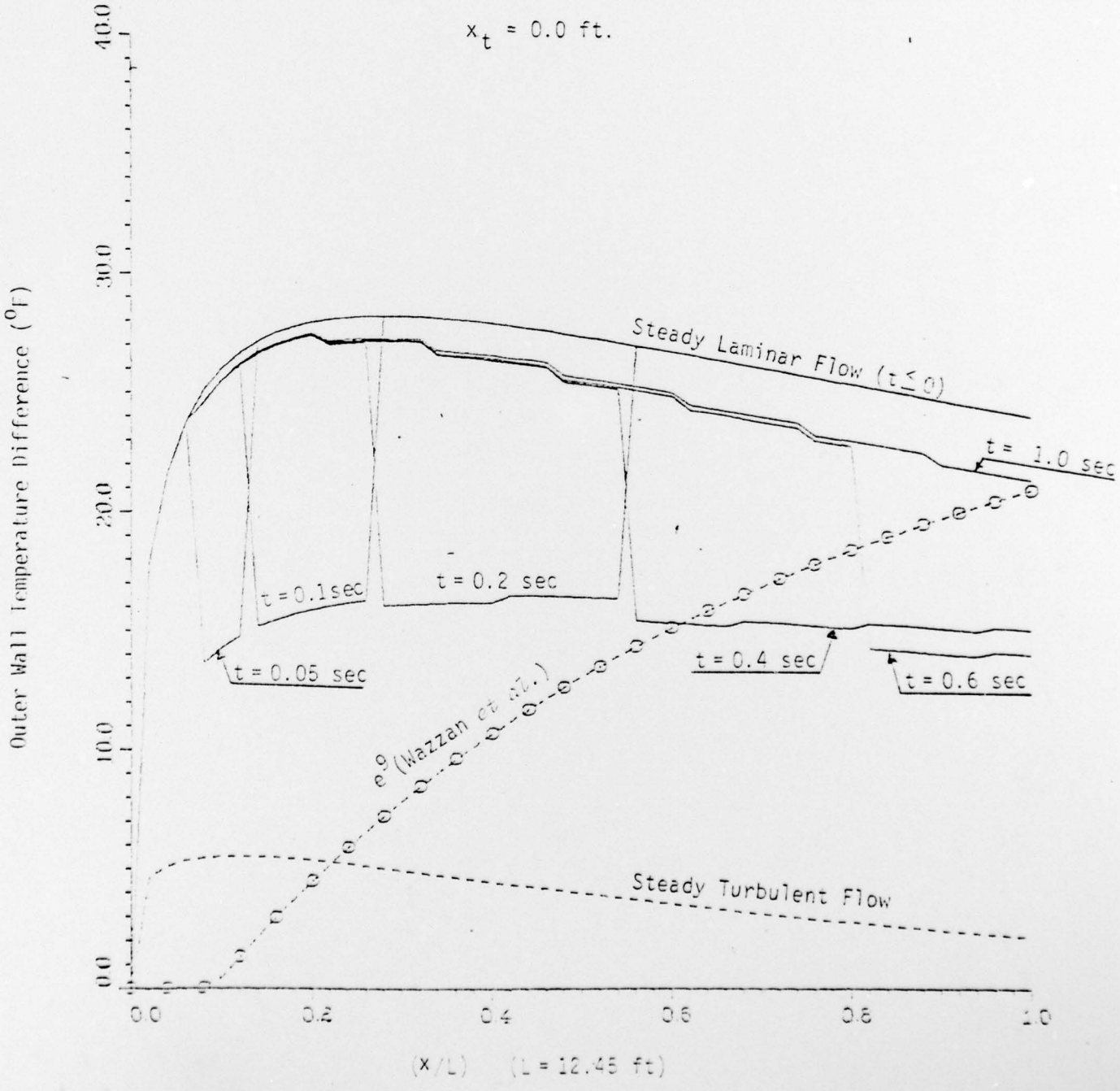

Figure 4.10 Recovery From a Single Turbulent Spot

$U = 40$ Knots (67.6 ft/sec)

$T_\infty = 70^0F$, $(\Delta T_i)_o = 95^0F$

$(x_t + 0.5\ Ut) \geq x \geq (x_t + Ut)$

$x_t = 0.0$ ft

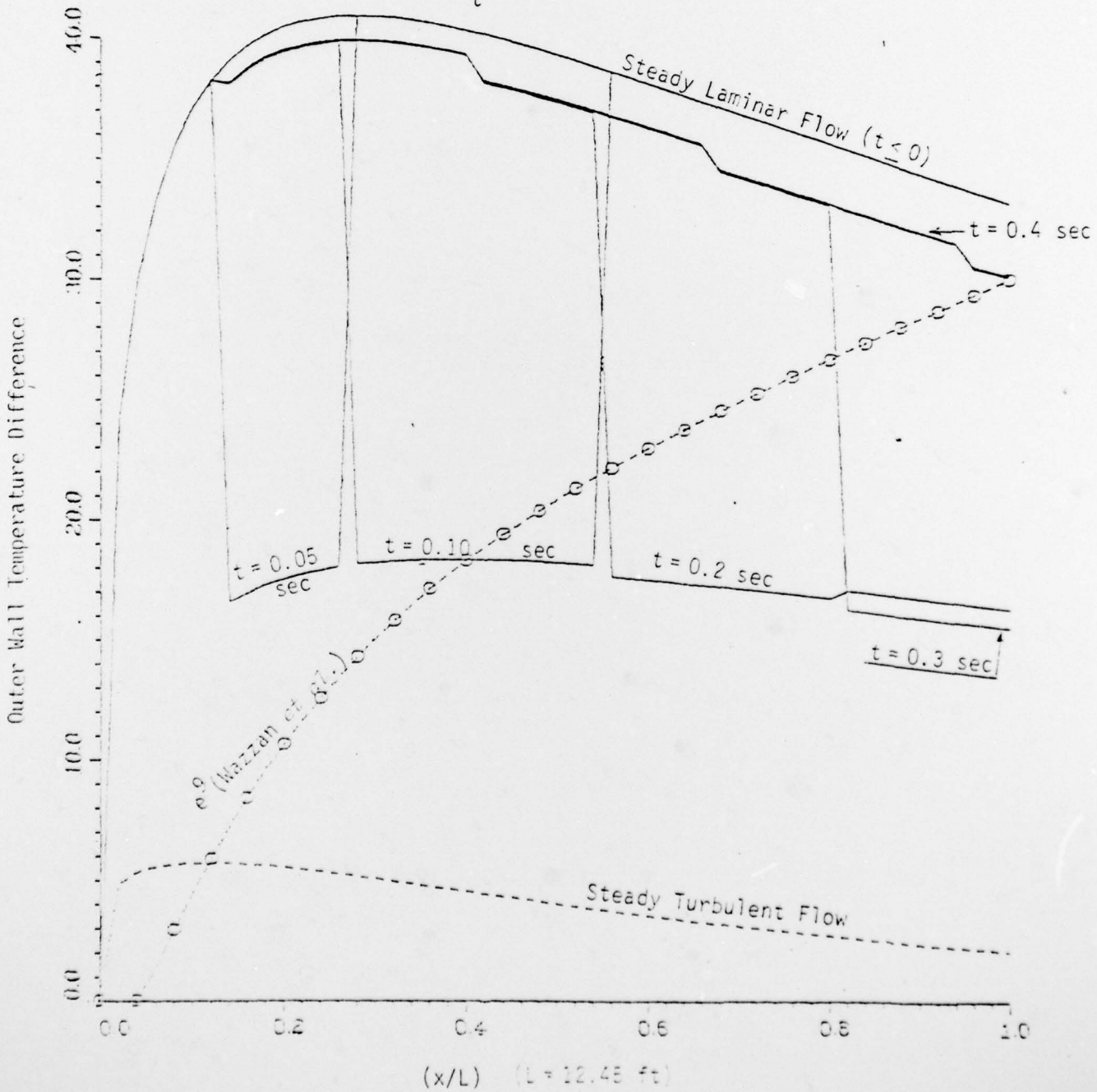

of these figures, the motion and streamwise growth of the turbulent spot can be easily visualized as can the effect on the wall temperature (the step-like appearance of the computed wall temperature distribution is not a manifestation of the numerical instability mentioned previously but, instead, is an artifact of the step-like manner - both in time and position - by which the finite difference equations are solved). Note that in both of the cases shown in Figures 4.9 and 4.10, the laminar boundary layer flow is fully re-established as soon as the turbulent spot is swept past the trailing edge.

If the particle entry/turbulent spot generation mechanism is, in fact, one whereby laminar flow could be temporarily lost (and there is some experimental evidence which substantiates this surmise) then it is very unlikely that only one such occurrence would be encountered. Instead, particles would be encountered at random time intervals distributed about a mean which is characteristic of their undisturbed spacing and the vehicle speed. Thus, a more realistic simulation of this mechanism would be to compute the effect of repetitive turbulence spots being swept over the flat plate surface. This was not done in the present study since a mean arrival rate could not be confidently estimated and because the two limiting cases of either a single particle or a continuous "swarm" of particle arrivals are contained in the calculations already described.

4.4 Time for Recovery of Laminar Flow

The process of recovering a fully laminar flow after experiencing turbulent events such as those described in Section 4.3 can be viewed in terms of the approach of $(\Delta T_w)_o$ to its steady laminar value. Consider the temperature distributions in the following sketch:

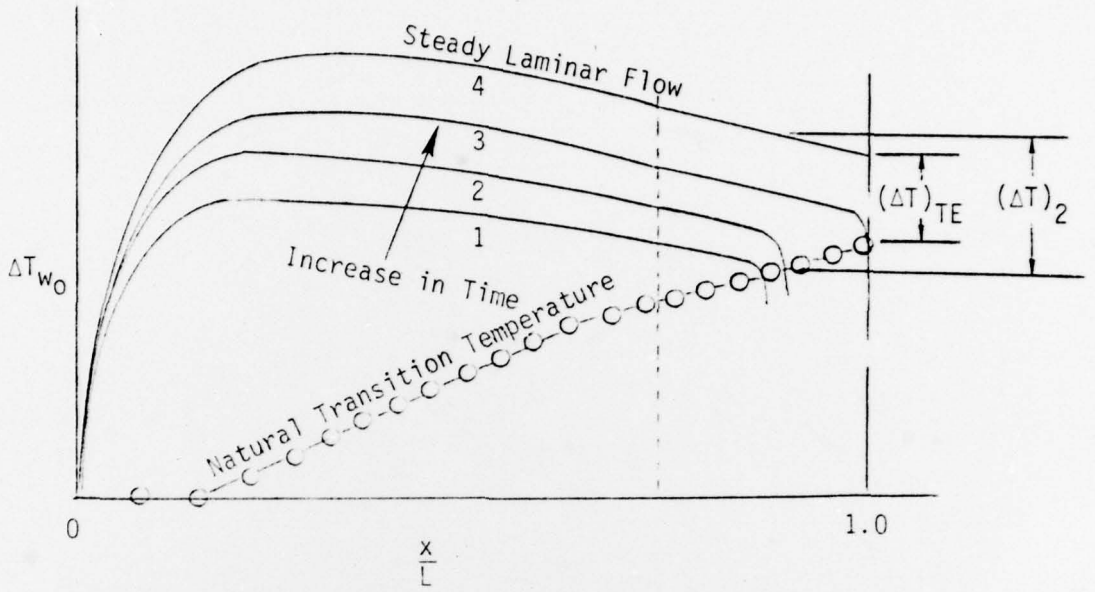

Temperature distribution 1 corresponds, say, to that at one of the calculated times. Temperature distribution 2 can be considered to be that at the last time where a reliable calculation is obtainable. Temperature distribution 4 is that for steady external laminar flow, and temperature distribution 3 is the earliest one for which the transition point reaches the end of the plate ($x/L = 1.0$). The recovery time can be estimated from the rate at which temperature profiles 1, 2 and 3 approach profile 4.

At any station x/L where the external flow is laminar (indicated by the vertical dotted line in the sketch), equations (3.21) and (3.22) for ΔT_i and ΔT_w can be written

$$\frac{\partial(\Delta T_i)}{\partial t} + \frac{u}{L} \frac{\partial(\Delta T_i)}{\partial \left(\frac{x}{L}\right)} = - H_1 (\Delta T_i) + H_2 (\Delta T_w) \qquad (4.1)$$

$$\frac{\partial(\Delta T_w)}{\partial t} = H_3 (\Delta T_i) - H_4 (\Delta T_w) \qquad (4.2)$$

where

$$\left.\begin{aligned} H_1 &= \frac{h_i}{\rho a c_i}\,(1-g_1) \\ H_2 &= \frac{h_i}{\rho a c_i}\,g_2 \\ H_3 &= \frac{\left[h_i(1-g_1) - h_i g_3\right]}{Mc_w} \\ H_4 &= \frac{\left[h_i g_2 + h_o g_4\right]}{Mc_w} \end{aligned}\right\} \qquad (4.3)$$

Near equilibrium (here represented by profile 4)

$$\left.\begin{aligned} \Delta T_i &= (\Delta T_i)_{eq} + \delta_i(t) \\ \Delta T_w &= (\Delta T_w)_{eq} + \delta_w(t) \end{aligned}\right\} \qquad (4.4)$$

Substituting relations (4.4) into equations (4.1) and (4.2) yields the following two sets of equations:

For the equilibrium distribution:

$$\left.\begin{aligned} \frac{u}{L}\,\frac{\partial(\Delta T_i)_{eq}}{\partial\left(\frac{x}{L}\right)} &= -H_1\,(\Delta T_i)_{eq} + H_2\,(\Delta T_w)_{eq} \\ H_3\,(\Delta T_i)_{eq} &= H_4\,(\Delta T_w)_{eq} \end{aligned}\right\} \qquad (4.5)$$

For the approach to equilibrium:

$$\left.\begin{aligned} \frac{\partial \delta_i}{\partial t} &= - H_1 \delta_i + H_2 \delta_w \\ \frac{\partial \delta_w}{\partial t} &= H_3 \delta_i - H_4 \delta_w \end{aligned}\right\} \qquad (4.6)$$

Equations (4.5) are, in fact, the equations for steady laminar flow whose solution would yield the temperature profile denoted as 4 in the previous sketch. Since the coefficients H_1, H_2, H_3 and H_4 are all constant, we seek solutions to equations (4.6) that are exponential in time.

Let $$\delta_i, \delta_w \sim e^{-\lambda t} \qquad (4.7)$$

Equations (4.6) then become

$$\left.\begin{aligned} (H_1 - \lambda)\delta_i - H_2 \delta_w &= 0 \\ H_3 \delta_i - (H_4 - \lambda)\delta_w &= 0 \end{aligned}\right\} \qquad (4.8)$$

For a non-trivial solution to these equations to exist, the quantity λ must satisfy the following equation

$$\lambda^2 - (H_1 + H_4)\lambda + (H_1 H_4 - H_2 H_3) = 0 \quad . \qquad (4.9)$$

The calculated values of λ for the three vehicle speeds considered are:

Table 4.3. Characteristic Time Constants

Freestream Speed (knots)	λ_1 (sec^{-1})	τ_1 (sec)	λ_2 (sec^{-1})	τ_2 (sec)
20	0.020	50	0.547	1.83
40	0.027	37	0.555	1.80
50	0.030	33	0.558	1.79

Only λ_1 and its reciprocal, the time constant τ_1, are relevant to the present problem since for $\lambda = \lambda_2$, the temperature deviations δ_i and δ_w are opposite in sign which is not appropriate for the recovery processes considered in this paper. For $\lambda = \lambda_1$, δ_i and δ_w have the same sign and in fact, for all the cases considered herein, the equilibrium laminar wall and heating fluid temperatures are both approached from below.

An analysis of the root λ_1 shows that to a very close approximation

$$\tau_1 \approx 1.12 \frac{(Mc_w + \rho a c_i)}{h_o} \tag{4.10}$$

indicating that the time constant is directly proportional to the heat capacity per unit area of the skin and heating fluid together and inversely proportional to the heat loss rate to the external flow.

The procedure for estimating the recovery time follows directly from Equation (4.7) and the sketch at the beginning of this section. One may write

$$\delta_w = \Delta T_{w_o} - (\Delta T_{w_o})_{laminar} \sim e^{-\frac{t}{\tau_1}} \tag{4.11}$$

More specifically, for the final calculated profile (profile 2) and the recovery profile (profile 3) we may write respectively

$$(\Delta T)_2 = A\, e^{-\frac{t_2}{\tau_1}}$$

$$(\Delta T)_{T.E.} = (\Delta T)_3 = A\, e^{-\frac{t_{recovery}}{\tau_1}}$$

or taking the ratio of the two temperature differences

$$\frac{(\Delta T)_{T.E.}}{(\Delta T)_2} = e^{-\frac{(t_{recovery} - t_2)}{\tau_1}} \tag{4.12}$$

where $(\Delta T)_3 = (\Delta T)_{T.E.}$ is the trailing edge wall temperature excess. Solving Equation (4.12) for the recovery time yields

$$t_{recovery} = \tau_1 \ln\left[\frac{(\Delta T)_2}{(\Delta T)_{TE}}\right] + t_2 \tag{4.13}$$

Note that when $(\Delta T)_{TE}$ goes to zero, the recovery time becomes infinite.

Recovery times have been estimated using Equation (4.13) for all the cases computed. Selected results related to the cases presented in Section 4.3 are given in the table below:

Table 4.4

RECOVERY TIMES

Speed (knots)	(ΔT_i) (^oF)	$(\Delta T_i)_{^oExcess}$ (^oF)	$(\Delta T)_{TE}$ (^oF)	Patch Length (ft)	$t_{Recovery}$ (sec)	
Recovery from a Long Turbulent Patch						
20	47.8	0	0	∞	∞	
	55	7.2	3.0		91	Figure 4.2
	60	12.2	5.2		69	Figure 4.3
40	86	0	0	∞	∞	
	90	4	1.4		107	
	95	9	3.1		80	Figure 4.4
50	105	0	0	∞	∞	
	115	10	3.2		76	
	120	15	4.8		64	
Recovery from a Finite Length Turbulent Patch Encounter						
20	55	7.2	3.0	67.6	66	Figure 4.5
				33.8	41	
				20.3	19	
40	95	9	3.1	135.2	72	
				67.6	53	Figure 4.6
				33.8	31	
Recovery from a Boundary Layer Trip ($x > 2$ ft)						
20	55	7.2	3.0		17	Figure 4.7
40	95	9	3.1		12	Figure 4.8

Recovery times are not given for the cases of the passage of a turbulent spot (Figures 4.9 and 4.10) since as has been noted earlier, laminar flow is recovered as soon as the turbulent spot is swept past the trailing edge.

In all cases, laminar flow is eventually recovered over the entire plate. As expected, the recovery time is a sensitive function of the trailing edge wall temperature excess and, therefore, also of the corresponding heating water inlet temperature excess. Recovery times can be reduced by providing a greater temperature excess.

Recovery times from exposure to finite length patches of turbulence are, of course, less than those for infinite patch lengths, but not a great deal less. This indicates that if a patch of turbulence extends for the order of three or more vehicle lengths, significant surface cooling occurs because of the turbulent, rather than laminar, external heat loss rate.

From momentary trips or turbulent spots, recovery is either instantaneous, or else the recovery times are fairly short, even shorter than indicated by the present calculations. This is because real trips and spots are three-dimensional (of finite spanwise extent) rather than two-dimensional as assumed in the calculations. The drag and heat transfer consequences of such disturbances are dependent more on their residence time (or flow time) and are only weakly dependent on the characteristic recovery times, τ_1, of Table 4.3.

5. CONCLUSIONS AND RECOMMENDATIONS

The maintenance of steady laminar flow on a heated submerged vehicle requires that the external skin temperature at every station on the vehicle be equal to or greater than that required to delay transition to that station. The ability of the vehicle to recover laminar flow after a turbulent event is sensitive to the amount by which the wall temperature exceeds the minimum required for laminar flow. If there is no temperature excess, the recovery time will be infinite. When there is excess temperature, the recovery time will depend on the extent to which the turbulent event has lowered skin temperatures, and is characterized by a time constant that is directly proportional to the heat capacity per unit area of the skin and heating fluid together and inversely proportional to the laminar heat loss rate to the external flow.

For the calculated cases, if a patch of turbulence extends for the order of three or more vehicle lengths, the recovery time for reasonable temperature excess is of the order of one to three characteristic times (1/2 to 2 minutes for the cases calculated). For momentary trips or turbulent spots, recovery occurs very soon after the spot or trip is swept past the trailing edge.

While, for simplicity, the vehicle of the present study has been modeled as a two-dimensional flat plate, the formulation is readily extendable to the geometries of actual test vehicles. It is strongly recommended that such analyses for actual geometries be carried out as part of the thermal design process of prospective vehicles and as an aid in the interpretation of test data. Attempts should be made to accommodate properly the three-dimensional character and azimuthal distribution of turbulent spots and momentary boundary layer trips.

REFERENCES

1. Reshotko, E., *"Drag Reduction in Water by Heating,"* Proceedings of Second International Conference on Drag Reduction, Paper E2, BHRA, 1977.

2. Smith, A.M.O., Wazzan, A.R. and Hsu, W.C., *"Laminarization of Bodies of Revolution Moving in Water,"* Report from UCLA (School of Engineering and Applied Science) dated October 1977.

3. Krieth, F., Principles of Heat Transfer, International Textbook Co., 1964.

4. Wazzan, A.R., Okamura, T.T. and Smith, A.M.O., *"The Stability and Transition of Heated and Cooled Incompressible Laminar Boundary Layers,"* Proc. of 4th Int'l. Heat Transfer Conf., Versailles, September 1970.

5. Eckert, E.R.G. and Drake, R.M., Jr., Heat and Mass Transfer, 2nd ed. McGraw-Hill, 1959.

DISTRIBUTION LIST FOR UNCLASSIFIED
TECHNICAL REPORTS ISSUED UNDER
CONTRACT N00014-77-C-0005 TASK NR 062-562

All addresses receive one copy unless otherwise specified.

Defense Documentation Center
Cameron Station
Alexandria, VA 22314 12 copies

Technical Library
David W. Taylor Naval Ship
Research and Development Center
Annapolis Laboratory
Annapolis, MD 21402

Library
Naval Academy
Annapolis, MD 21402

Dr. Philip A. Selwyn
DARPA/TTO
1400 Wilson Boulevard
Arlington, VA 22209

Office of Naval Research
Code 211
800 N. Quincy Street
Arlington, VA 22217

Office of Naval Research
Code 438
800 N. Quincy Street
Arlington, VA 22217 3 copies

NASA Scientific and Technical
Information Facility
P. O. Box 8757
Baltimore/Washington Inter-
national Airport
Maryland 21240

Dr. Steven J. Barker
Poseidon Research
11777 San Vicente Boulevard
Los Angeles, CA 90049

Mr. Roy Gulino
Westinghouse Electric Corp.
Oceanic Division
Box 1488
Annapolis, MD 21404

Librarian
University of California
Dept. of Naval Architecture
Berkeley, CA 94720

Library (Code 5641)
Dr. W. E. Cummins, Code 15
Dr. J. H. McCarthy, Code 1552
David W. Taylor Naval Ship Research
and Development Center
Bethesda, MD 20084 3 copies

Professor P. Leehey
Massachusetts Institute of Technology
Department of Ocean Engineering
Cambridge, MA 02139

Library
Naval Weapons Center
China Lake, CA 93555

Professor E. Reshotko
Case Western Reserve University
Div. of Chemical Engineering Science
Cleveland, OH 44106

Technical Library
Naval Weapons Surface Center
Dahlgren Laboratory
Dahlgren, VA 22418

Mr. Dennis Bushnell
NASA Langley Research Center
Langley Station
Hampton, VA 23365

Professor L. Landweber
Institute of Hydraulic Research
University of Iowa
Iowa City, IA 52242

Mr. Carl G. Jennings
Rockwell International Corp.
Autonetics Group
Anaheim, CA 92803

Distribution List (Cont.)

Fenton Kennedy Document Library
The Johns Hopkins University
Applied Physics Laboratory
Johns Hopkins Road
Laurel, MD 20810

Dr. S. Orszag
Cambridge Hydrodynamics, Inc.
54 Baskin Road
Lexington, MA 02173

Professor Tuncer Cebeci
California State University
Mechanical Engineering Dept.
Long Beach, CA 90840

Dr. T. D. Taylor
The Aerospace Corporation
P. O. Box 92957
Los Angeles, CA 90009

Lorenz G. Straub Library
St.Anthony Falls Hydraulic Lab.
University of Minnesota
Minneapolis, MN 55414

Library
Naval Postgraduate School
Monterey, CA 93940

Technical Library
Mr. Fred White, Code 36301
Mr. Richard Nadolink, Code 3635
Naval Underwater Systems Center
Newport, RI 02840 3 copies

Professor H. W. Liepmann
Graduate Aeronautical Laboratories
California Institute of Technology
Pasadena, CA 91109

Dr. Leslie M. Mack
Jet Propulsion Laboratory
California Institute of Technology
Pasadena, CA 91125

Technical Library
Dr. George L. Donohue, Code 6302
Dr. Michael M. Reischman, Code 6342
Dr. James Logan, Code 631
Naval Ocean Systems Center
San Diego, CA 92132 4 copies

Dr. Carl Gazley, Jr.
The Rand Corporation
1700 Main Street
Santa Monica, CA 90406

Librarian
Naval Surface Weapons Center
White Oak Laboratory
Silver Spring, MD 20910

Dr. D. R. S. Ko
Dynamics Technology, Inc.
3838 Carson Street, Suite 110
Torrance, CA 90503

Dr. Phillip S. Klebanoff
National Bureau of Standards
Mechanics Division
Washington, DC 20034

Dr. Robert J. Hansen
Naval Research Laboratory
Code 2627
Washington, DC 20375

Library (Code 09GS)
Dr. E. G. Liszka, Code 03421
Dr. Thomas E. Pierce, Code 03512
Mr. R. Manning, Code 395A
Naval Sea Systems Command
Washington, DC 20362 4 copies

Professor Blaine R. Parkin
Dr. G. C. Lauchle
Pennsylvania State University
Applied Research Laboratory
University Park, PA 16802 2 copies